Evidence for pre-folding vein development in the Oligo-Miocene Asmari Formation in the Central Zagros Fold Belt, Iran

Faram Ahmadhadi[1], Jean-Marc Daniel,[2] Mehran Azzizadeh,[3] and Olivier Lacombe[4]

Received 8 April 2007; revised 11 October 2007; accepted 29 October 2007; published 27 February 2008.

[1] In order to understand the interplay between vein development and folding in the carbonates of the Oligo-Miocene Asmari Formation (one of the main hydrocarbon reservoir rocks) in Iran, several anticlines have been investigated in the central part of the Zagros folded belt. Combining observations of relative chronology between veins based on calcite-filling phases and crosscutting/abutting relationships, as well as aerial/satellite image interpretation on several anticlines allowed proposing a tectonic model highlighting the widespread development of veins and other extensional micro/meso-structures in the Central Zagros folded belt. Our data suggest that most of the veins affecting the Asmari formation predated the main Miocene-Pliocene folding episode. An early regional vein set striking N50° marked the onset of collisional stress build-up in the region. Then, N150° and N20° trending vein sets were initiated in response to local extension caused by large-scale flexure/drape folds above N-S and N140° basement faults reactivated under the regional NE compression. At the onset and during Miocene-Pliocene folding of the sedimentary cover, the early formed veins were reactivated (reopened and/or sheared) while duplexes, low angle reverse faults and thrusts formed. Beyond regional implications, this study puts emphasis on the need of carefully considering regional/local vein development predating folding as well as influence of underlying basement faults in models of folded-fractured reservoirs in fold-thrust belts. **Citation:** Ahmadhadi, F., J.-M. Daniel, M. Azzizadeh, and O. Lacombe (2008), Evidence for pre-folding vein development in the Oligo-Miocene Asmari Formation in the Central Zagros Fold Belt, Iran, *Tectonics*, *27*, TC1016, doi:10.1029/2006TC001978.

1. Introduction

[2] The understanding of the factors that control the characteristics of fracture patterns, such as orientation distribution, density spatial variation and chronology is fundamental to improve the methods used to characterize fractured reservoirs. Furthermore, from a regional-scale point of view, this understanding is of major interest for development plans of these reservoirs, which can constitute petroleum provinces like the Southwest Zagros. Fold geometry and kinematics are well known to be important factors that control fracturing. Therefore many studies have tried to relate development of micro and meso-structural pattern to fold geometrical elements, such as fold axis, forelimb, backlimb and termination [*McQuillan*, 1974; *Srivastava and Engelder*, 1990; *Cooper*, 1992; *Fischer et al.*, 1992; *Erslev and Mayborn*, 1997; *Jamison*, 1997; *Thorbjornsen and Dunne*, 1997; *Hennings*, 2000]. The paper published by Stearns in 1972 should be mentioned as the synthesis of the pioneering work done on this topic. This synthesis is presented in the form of a classification of fractures (including joints and faults) based on their position with respect to the characteristic geometrical elements of folds. This famous scheme of fractures population in a typical anticline including axial, transversal and oblique fractures, was essentially static and tried to emphasize the relationship between typical fracture populations and their location in a fold according to the present-day shape of the fold. Then it was followed by the quantitative characterization of fold geometry using curvature [*Lisle*, 2000]. Curvature is still used frequently as a tool to define fractures direction and intensity [*Hennings*, 2000; *Bergbauer and Pollard*, 2004]. However, in the recent years, due to the development of kinematic models of folding, several attempts have been made to relate fracturing to the kinematics of folds instead of looking simply at the final shape of the folds in accordance with the observations that fracturing records a progressive deformation during folding [*Allmendinger*, 1982; *Couzens and Dunne*, 1994; *Fisher and Anastasio*, 1994; *Anastasio et al.*, 1997; *Storti and Salvini*, 2001; *Tavani et al.*, 2006].

[3] Because of the important role of fractures in the hydrocarbon production from the Dezful Embayment (Southwest Zagros) oil fields, many studies have been done in this area to describe the fracture population within carbonate reservoirs since 1940 [see *Motiei*, 1995 for a review]. Among the studied formations, the Asmari Formation is famous with regards to fracture studies because (i) this Oligo-Miocene Formation spectacularly crops out in a 1200 km long by 200 km wide belt extending from northeast Iraq to southwest Iran [*Beydoun*, 1988], (ii) it contains a lot of the hydrocarbon reserves of this area and (iii) it produces mainly via fractures due to the generally tight matrix [*Hull and Warman*, 1970]. Using aerial photos

[1]Iranian Offshore Oil Company (IOOC), Geology & Petrophysics Department, Tehran, Iran.
[2]Institut Français de Pétrole (IFP), Rueil-Malmaison Cedex, France.
[3]RIPI, West Blvd., Azadi Sports Complex, Tehran, Iran.
[4]Université P. & M. Curie - Paris 6, Laboratoire de Tectonique, UMR 7072 CNRS, Paris Cedex, France.

0278-7407/08/2006TC001978$12.00

and outcrop observations, *McQuillan* [1973, 1974] demonstrated that fracture population in this area is consistently defined by three sets trending N20°–30°E, N80°E, and N160°–170°E and suggested that these sets bear no relation to the geometry of folds formed during the Mio-Pliocene Zagros orogeny. In contrast with McQuillan, *Gholipour* [1998] claimed that fractures in the Asmari reservoirs are associated with vertical and axial growth of concentric folding, which means that they are mostly fold-related. This conclusion was however mainly based on the study of well data (well-tests, production logs, mud losses) in some of the Asmari fields.

[4] The aim of this paper is to take advantage of the outstanding quality of the Zagros outcrops and of the existing studies to present new observations that can be used to discuss the relationships between development of the fracture network and folding. The fact that contractional tectonics shortly postdates deposition of the Asmari formation is an interesting characteristic of this area with respect to this objective, because the observed structures cannot be related to many tectonic events but rather to the progressive deformation related to the Zagros orogeny. Special attention has been paid to accurately characterize the types of fractures and their chronology with respect to folding, in order to test various existing models of relationships between fracturing and folding and to establish a link between this chronology and the regional tectonic evolution. Analysis of high resolution satellite and aerial images was used as a complementary tool to define the trends of large-scale faults and fractures. The results of our analysis are synthesized in the form of a conceptual model that highlights (1) that most extensional fractures are veins that were created before folding and (2) that most of them were later reactivated during generalized folding of the Zagros cover in response to the Mio-Pliocene paroxysm of Arabia-Eurasia collisional shortening.

2. Geological Setting

2.1. Tectonic Setting

[5] The present morphology of the Zagros is the result of a geological history including a platform setting during the Paleozoic; a Tethyan rifting phase in the Permian-Triassic; a passive continental margin setting (with seafloor spreading to the northeast) in the Jurassic-Early Cretaceous; Tethyan subduction to the north-east and obduction in the Late Cretaceous; and finally Arabia-Eurasia collision during the Neogene [*Falcon*, 1974; *Berberian and King*, 1981; *Berberian*, 1983; *Agard et al.*, 2005]. The Zagros is a young (Mio-Pliocene) NW-SE to nearly E-W (in its SE part) trending fold-thrust belt located along the northern margin of the Arabian Plate. This belt is currently undergoing 20–25 mm/a shortening [*Jackson and McKenzie*, 1984; *DeMets et al.*, 1990; *McClusky et al.*, 2003; *Vernant et al.*, 2004] and thickening as a result of collision of the Arabian and central Iran plates [*Berberian and King*, 1981; *Berberian*, 1983]. This belt provides a good example of convergence partitioning in its NW part, the overall N-S convergence between the Arabian and Eurasian plates being accommodated by dextral strike-slip movement at the rear of the belt along the Main Recent Fault (MRF) [*Talebian and Jackson*, 2002] and by belt-perpendicular shortening leading to the formation of N140° trending folds [*Hessami et al.*, 2001; *Agard et al.*, 2005; *Vernant and Chery*, 2006].

[6] The Zagros folded belt has been divided into several morphotectonic regions [*Falcon*, 1961; *Haynes and McQuillan*, 1974; *Berberian*, 1995] (Figure 1b). These main morphotectonic regions are limited by deep-seated basement faults [*Berberian*, 1995]. Two dominant tectonic trends, respectively N-S and NW-SE, are well known in the Arabian Shield and there is evidence for the continuation of these trends northward into the Zagros belt [*Berberian*, 1995; *Talbot and Alavi*, 1996; *Hessami et al.*, 2001; *Bahroudi et al.*, 2003]. In the Zagros belt, the approximate locations and geometries of the basement faults have been defined using geodetic survey, more or less precise epicenter/hypocenter locations, as well as topographic and morphotectonic analyses [*Berberian*, 1995]. The first group of basement faults includes the Mountain Front fault (MFF), the Dezful Embayment fault (DEF), and the Zagros Foredeep fault (ZFF) (Figure 1b). Fault plane solutions for earthquakes along these faults indicate that they all dip about 60°NE, suggesting that they now act as reverse faults although they may have acted as normal faults during the Permo-Triassic opening of Neo-Tethys [*Jackson*, 1980; *Berberian*, 1995]. Another group of basement faults are N-S trending faults which developed during the latest Proterozoic and early Cambrian in the Arabian basement [*Beydoun*, 1991]. During the Mesozoic, and especially in the Triassic and Late Cretaceous, N-S trending uplifted zones and basins were related to the intermittent reactivation of this group of basement faults [*Motiei*, 1995; *Sherkati and Letouzey*, 2004]. These faults are steeply dipping and currently undergo right-lateral strike-slip motion [*Berberian*, 1995; *Hessami et al.*, 2001; *Sepehr et al.*, 2002]. Some of these faults, located in the studied area, are the Izeh-Hendijan Fault (IZHF), the Kharg-Mish Fault (KMF) and the Kazerun Fault (KZ) (Figure 1b). The Balarud Fault (BR) is an E-W left-lateral shear zone northwest of the Dezful Embayment. The activity of Kharg-Mish fault (KMF), based on thickness and facies variations seen in wells, started after Lower Aptian time. Structural information derived from seismicity within the Zagros belt [*Jackson and McKenzie*, 1984; *Ni and Barazangi*, 1986; *Berberian*, 1995; *Talebian and Jackson*, 2002, 2004] proves that these faults are still active as right-lateral strike-slip faults in the basement underlying the folded cover.

[7] The area studied in this paper covers part of the southwestern margin of the Izeh zone and the northeastern margin of the Dezful Embayment (Figure 1b). The Izeh zone is part of the Zagros folded belt: it is limited to the north-northeast by the High Zagros Fault (HZF), to the south-southwest by the Mountain Front Fault (MFF), and to the northwest by the Balaroud flexure (BF). The Dezful Embayment primarily corresponds to a morphotectonic region stepped down with respect to the Izeh zone, surrounded by three of the major basement structures described above. The north-northwestern limit is the Balaroud flexure, the east-northeastern limit is the Mountain Front Fault

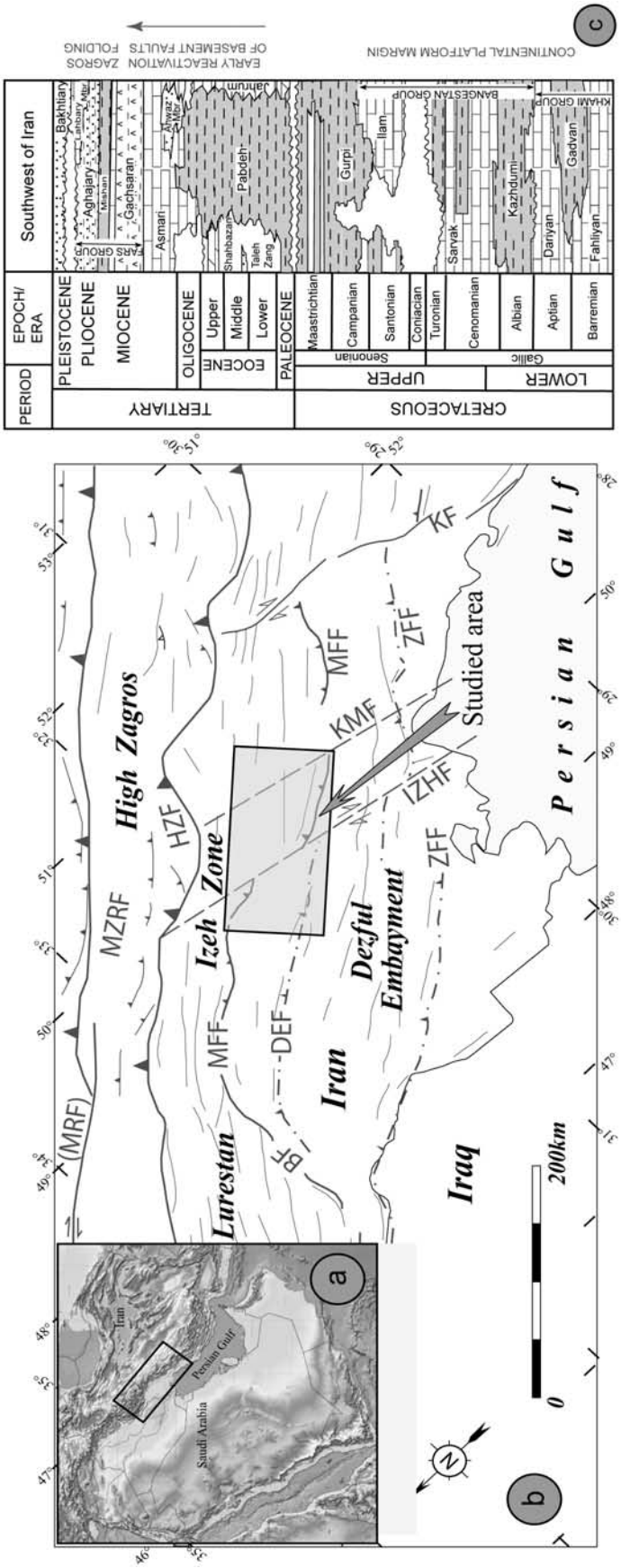

Figure 1. (a) Location map and (b) main morphotectonical divisions [*Haynes and McQuillan*, 1974; *Favre*, 1975; *Motiei*, 1993]. (c) Lithostratigraphy in the studied area since Lower Cretaceous [after *James and Wynd*, 1965].

(MFF) and its south-southeastern limit is the Kazerun Fault [*Sepehr and Cosgrove*, 2004].

2.2. Lithostratigraphy

[8] Generally three main lithological series are exposed in this area from Lower Cretaceous up to Pliocene (Figure 1c); (i) Carbonate series, including part of the Khami Group (Fahliyan and Dariyan Formations, of Neocomian and Aptian age, respectively), Ilam and Sarvak Formations (Cenomanian to Santonian) and the Asmari Formation (Oligocene-Lower Miocene); they form the main reservoir rocks in southwest Iran. (ii) Clastic and argillaceous series, including the Gadvan Formation of the Khami Group (Neocomian-Aptian), Kazhdumi (Albian), Gurpi (Campanian-Maastrichtian), Pabdeh (Paleocene-Eocene), Mishan, Agha-Jari and Bakhtiary Formations (Upper Miocene-Lower Pleistocene). Kazhdumi and Pabdeh Formations are well known as petroleum source rocks in the region. (iii) Evaporitic series, including the Kalhur member (Lower Miocene?) within the Asmari Formation and the Gachsaran Formation (Middle Miocene), which is the main caprock of the Asmari reservoirs in Iran. All the above sedimentary series more or less crop out in the Izeh part of the studied area, whereas the most part of the Dezful Embayment is covered by Middle Miocene to recent sediments. However, near the north-north-eastern margin of the Dezful embayment and south of the Mountain Front Fault, the Asmari Formation crops out in anticlines that are sometimes cored by the Pabdeh Formation (e.g., Asmari, Khaviz, Dil and Pahn anticlines in Figure 2). The Asmari type section was described initially by R.K. Richardson and Thomas (cited in *Motiei*, 1995) in Gel-e Torsh valley in the Asmari anticline located in this zone (west of the area covered by Figure 2). This type section is 314 m thick and consists mostly of dense, cream to brown colored limestones and some shaly beds.

2.3. Structural Style

[9] The sedimentary column in the Zagros is estimated to be up to 12 km thick and a great part of this column was supposed to have been folded as a single competent group [*James and Wynd*, 1965; *Falcon*, 1974]. This competent group includes sediments ranging from Cambrian to Miocene. It is embedded between two main detachment levels (mobile groups): the Hormuz Salt Formation (Infra-Cambrian) at the base, and the Gachsaran Formation (Lower Miocene) at the top [*Lees*, 1952; *Falcon*, 1974; *Colman-Sadd*, 1978]. The basement is thought either to have remained rigid or, more likely, to have undergone block faulting [*Lees*, 1952; *Falcon*, 1974; *Talebian and Jackson*, 2004]. From a geometrical point of view, most of the folds in the Central Zagros are asymmetric and, with a few exceptions, the steepest limbs of the anticlines are on the southwest sides. The most likely mechanism to explain this regionally consistent asymmetry is shearing in the decollement level of the lower mobile group [*Colman-Sadd*, 1978]. The depth of this basal decollement is not clear through seismic data within the Izeh zone and the Dezful Embayment. It has been considered to be at a minimum of 9000–10,000 m below see level in the Dezful Embayment based on the thickness of the sedimentary sequence and the largest wavelength of the folds [*Letouzey et al.*, 2002]. In this context, parallel (buckle) folding in the Zagros have been introduced as essential fold geometry based on mechanical stratigraphy of the area [*Colman-Sadd*, 1978], folds aspect ratio (half wavelength to axial length ratio) and spatial organization [*Price and Cosgrove*, 1990]. In the competent group, flexural slip has been described as associated to buckling [*Colman-Sadd*, 1978]. In addition to buckle folds, forced folds have been described in the Zagros fold belt and many of them are linked to underlying thrusts [*Sattarzadeh et al.*, 2000]; these (often high angle) thrusts are thought to have developed in response to the reactivation of basement normal faults during (and subsequent to) the major collisional Miocene-Pliocene episode.

[10] Recent studies have revealed that a single basal decollement is not sufficient to explain the shape of the Zagros folds. Consequently, the presence of intermediate incompetent layers within the sedimentary succession and their role on folding style have been discussed by different authors [*Blanc et al.*, 2003; *Sepehr and Cosgrove*, 2004; *Sherkati and Letouzey*, 2004]. The presence of short wavelength anticlines in the Oligo-Miocene Asmari Formation in the Izeh zone supports for example that Pabdeh and Gurpi formations are efficient intermediate décollement levels in this area whereas this role is played by the Albian shales of the Kazhdumi Formation in the southeast of the Izeh zone and parts of the northeast Dezful Embayment [*Sherkati et al.*, 2006]. These intermediate décollements strongly influence the kinematics of folding since thrusts progressively propagate into upper décollement levels through time inducing successive reduction in the anticline wavelength. These observations are in line with numerical and analogue models showing how multiple decollements, their spatial distributions, their thickness and their competence relative to the competence of rigid layers can affect this kinematics [*Dahlstrom*, 1990; *Couzens-Schultz et al.*, 2003; *Koyi and Vendeville*, 2003; *Sherkati et al.*, 2006]. Furthermore, the geometry of footwall synclines, of thrusts and the amount of limb rotation are best explained by a transition from decollement folding to fault-related folding [*Sherkati and Letouzey*, 2004].

[11] At the regional scale, the amount of shortening and the inter-limb angle in the folds decrease from NE to SW within Izeh zone (with a mean shortening of about 16%) and Dezful Embayment (with a mean shortening of about 6%) [*Sherkati and Letouzey*, 2004]. Figure 3 shows the typical deformation style with thrusts and detachment levels playing an important role on the structural evolution and fold geometry.

[12] In addition to thrusts and décollement levels, the N-S striking faults (i.e., IZHF, KMF) significantly control the deformation pattern at a large scale. These lineaments are strongly oblique to the Zagros trend and they affect the axial trends of the overlying folds (e.g., Bangestan anticline, Figure 2).

3. Data Collection and Analysis

3.1. Sampling Strategy

[13] In order to study the genetic relationship between folding and the observed structures, the current practice in

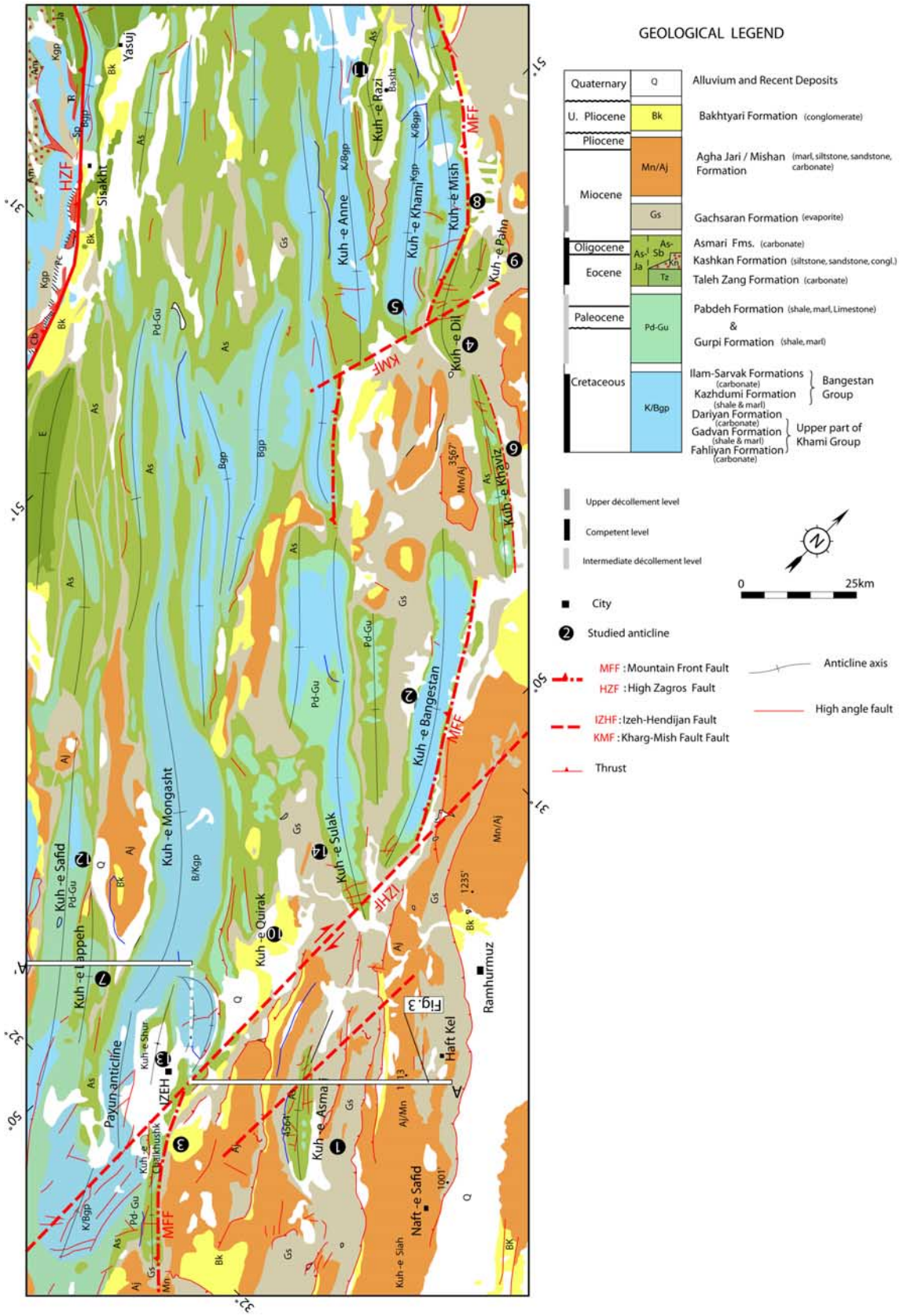

Figure 2. Simplified geological map of the studied area (modified from NIOC 1/1000,000 scale geological map of south-west Iran). The location of the structural transect (line AA′: Figure 3) is shown.

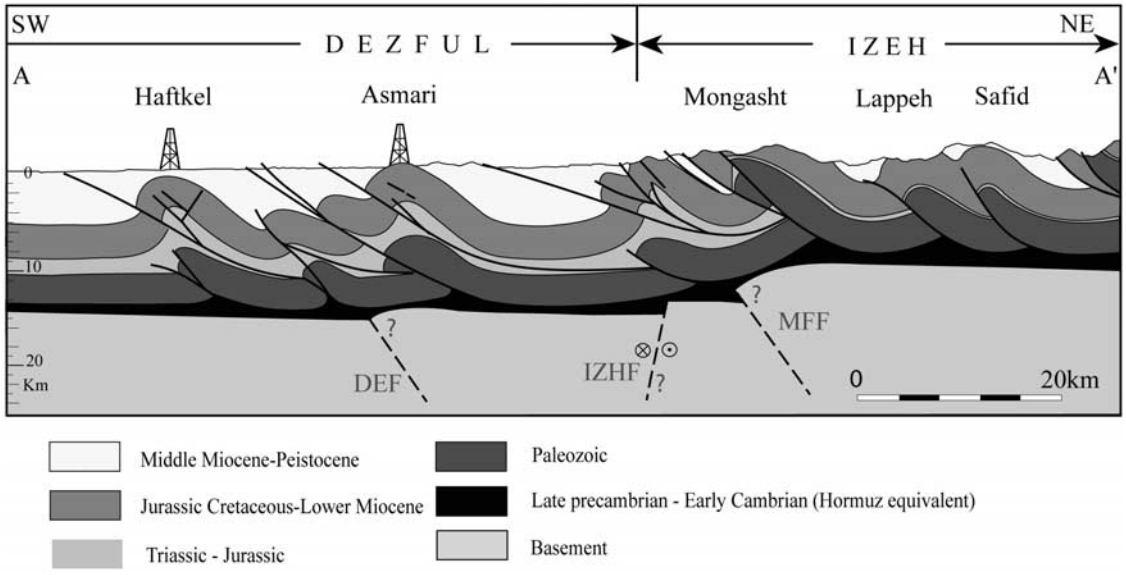

Figure 3. Regional transect through the studied area showing regional deformation style in the Izeh zone and the north of Dezful Embayment (line AA′ in Figure 2). Important basement features, Mountain Front Fault (MFF), Dezful Embayment Fault (DEF), and dextral strike-slip Izeh-Hendijan Fault (IZHF) are seen in this transect [modified from *Sherkati et al.*, 2006].

structural geology is to map the micro- and/or meso-structure orientations and densities in several sites distributed over one fold [*Hennings*, 2000; *Silliphant et al.*, 2002; *Tavani et al.*, 2006 for examples]. The analysis of the spatial distribution of these two quantities between the different fold sectors or their correlation with geometrical attributes such as dip and curvature can then be used to discuss the relationship between the development of the studied structural fabric and folding. In addition, these data can be compared with those coming from areas remained undeformed by folding [*Bergbauer and Pollard*, 2004; *Cooper et al.*, 2006]. Finally, such data set is generally completed with observations concerning the chronology between the various observed structures, cement filling, and evidence for reactivation.

[14] The geological evolution of the Dezful embayment shows evidence of interactions between basement faulting and cover folding during and after deposition of the Asmari carbonates in the Zagros foreland [e.g., *Ahmadhadi et al.*, 2007]. Therefore before rushing to the detailed description of a single fold, the data collection was organized to cover a large area (approximately 100 * 200 km^2) and several folds in order to be able to differentiate regional trends from fold-related ones (Figure 2). Without such regional understanding there is a great risk to misinterpret observations made at a more local scale. To achieve this objective, in each measurement sites (approximately 50 * 50 m^2), micro/mesostructures affecting the Asmari Formation were carefully characterized in terms of type and origin, orientation and chronological relationships (see below). This results in a data set of 88 observation sites. Among the studied outcrops, five anticlines are presented in more detail in this paper. In the Asmari anticline, structural measurements were carried out on different structural positions, including SE nose, crest and SW flank. In the Bangestan and Khaviz anticlines, these measurements were restricted on their SE noses. In Kuh'e Safid the NE flank was studied. Finally a complete transverse cross section was analyzed in the Razi anticline.

[15] In this first step, no density data were collected because (i) this was not possible in the time frame of the three surveys aiming at covering the area of interest, (ii) at regional scale the factors that can control fracture density are much more numerous than at a fold scale (e.g., mechanical stratigraphy, burial curves, petrophysical characteristics show much larger variation than at the fold scale) requiring even more data to be conclusive, (iii) the site description presented above provides the information necessary to select an anticline suited for further detailed analysis of micro/meso-structure density. Though density data will be collected in a next future, it appears from the analysis of the studied sites that many first-order characteristics concerning fracturing in the Asmari limestones were captured. This is certainly due to the large size of the area and to the significant variety of the structural positions covered by sites documented with structure types, orientations and chronology. Description and discussion of these first-order characteristics are the main objectives of this paper.

3.2. Observation and Characterization of Microstructures

[16] The more numerous structures observed in outcrops are rectilinear fractures, with a regular spacing and a significant length (3 to a few tens of meters) (see Figures 5a, 5b, 9). These fractures show opening displacement with no observ-

able shear movements (e.g., N140° vein on Figure 5c for example). Some of them show only microscopic opening displacement and can be classified as joints [p. 33 *Engelder*, 1987] but most of them are veins [*Engelder*, 1987, p. 42] characterized by various thickness of cement. When their wall are exposed due to variable amount of cement remains, plumose structures/hackle marks, i.e., common and characteristic features of mode I fractures [*Engelder*, 1987; *Pollard and Aydin*, 1988], are sometimes preserved (Figure 5a). In practice in the field, as noticed by example by *Graham Wall et al.* [2006], the distinction between joints and veins by the naked eyes can be ambiguous when veins are thin or partly weathered. In addition, we must keep in mind that a vein can correspond to a joint reopened by successive tectonic episodes (e.g., Figure 5g).Consequently, joints and veins in the Asmari limestones have been treated the same in the structure orientation analysis in accordance with their common opening mode origin [*Engelder*, 1987], but the distinction was kept as often as possible in the description of the various sites. In most sites thin sections were cut in order to check the mode of formation together with the possible occurrence of multiple cementations and therefore of successive increments of vein opening/re-opening (Figure 5g); it is however beyond the scope of this study to describe in detail the nature of cements and the evidence of vein-rock interactions observed in thin sections.

[17] In many of the studied outcrops, small shear displacements (Figure 5d), splay veins (Figure 5e) and extensional jogs were observed along veins. Such fractures will be called sheared veins [*Engelder*, 1987; see also *Peacock and Sanderson*, 1995]. In addition, faults have been observed in all surveyed sites. The more frequent are normal faults, followed by strike-slip ones that are themselves more frequent that reverse faults. Bedding-parallel slip is also frequently seen, demonstrating that flexural slip is one important deformation mechanisms in Zagros folds. Unfortunately, on the vast majority of the surfaces along which displacements have been observed, kinematics indicators (mostly calcite steps and stylolite striations when observed) have been obliterated by weathering. Therefore these kinematic data that were systematically collected are still too scarce to be used for a significant quantitative kinematic analysis at the regional scale.

[18] Finally, bed-parallel stylolites are also frequently observed. Tectonic stylolites (oblique or perpendicular to bedding plane) are less frequent (Figure 5f). They are absent of many of the studied sites and only a very few of them show a significant density of these structures (spacing in the range of one meter). Therefore their quantitative analysis deserves further acquisition of additional data at a higher resolution (at the fold scale). We acknowledge that such analysis could bring key constraints on fold kinematics but from a regional scale perspective we will mainly focus on veins that are clearly the main microstructures affecting Asmari carbonates.

3.3. Statistical Analysis of Measurement Data

[19] All orientation data were acquired using electronic compasses (TECTRONIC 4000). The measurement sites were selected either along an entire section of the Asmari Formation, on structural surfaces at the top of the Asmari Formation, or in a single position where it was possible to limit the bias due to outcrop orientation. In most of the measurement stations the bedding thickness was in the range of 20 cm to 200 cm. In the following, orientations data are presented in form of lower hemisphere stereodiagrams using Schmidt projection. On the synthetic map of Figure 12a, individual measurement sites located close to each other and in a similar structural position in the fold, and which led to similar observations were gathered in order to reduce the number of diagrams.

[20] As discussed in subsection 3.2, veins are the main structures that were analyzed in term of orientation sets. Members of a vein set share a common range of strike and dip orientation. In order to perform a statistical analysis of orientation data, an original method for the automatic definition of oriented data clusters was used. The density of oriented data represented as poles on a polar diagram is estimated at each point of the sphere using an Epanechnikov kernel. Outliers are removed by filtering, and the density distribution is smoothed by manually changing the variance of the kernel [*Wollmer*, 1995]. In a first step, cluster centers are identified by searching for local maxima of the density map using the method introduced by *Kittler* [1976]. This step results in the definition of a number of clusters and a guess for the mean pole of each cluster. This guess allows each vein to be classified probabilistically using its distance from each cluster center. Then the algorithm presented by *Marcotte and Henry* [2002] is used to finalize the vein set classification. This method is based on the assumption of a bivariate normal distribution of the veins within a set. This analysis has been applied to orientation data set containing between 50 to 200 veins with a length greater than 50 cm randomly sampled in each site. The results of this analysis are presented in a polar stereonet using the Schmidt projection on the lower hemisphere with great circles representing the mean plane of each vein set and contours representing the density distribution of the vein poles. As the vein sampling was not systematic along scanlines or surfaces, we are aware that these density distributions should be interpreted with caution. However, when a set is clearly over sampled with respect to the others, there is a high probability that it corresponds to the denser one, especially if this is consistently observed in nearby sites.

[21] In each surveyed site, bedding planes were also systematically measured in order to represent the collected orientation data in both their present-day and in their unfolded attitudes. To unfold the orientation data, we assumed that the sites did not suffer any rotation around a vertical axis and that the local fold axis is horizontal. If the latter is a reasonable hypothesis because the dip of the fold axis in the studied area never exceeds 10°, the former could be discussed for some of the sites, especially for those located along the N-S trending lineaments. Following these hypotheses, the fracture data were unfolded using the rotation necessary to bring the average bedding back to a horizontal attitude. Maps of ''folded'' and ''unfolded'' vein

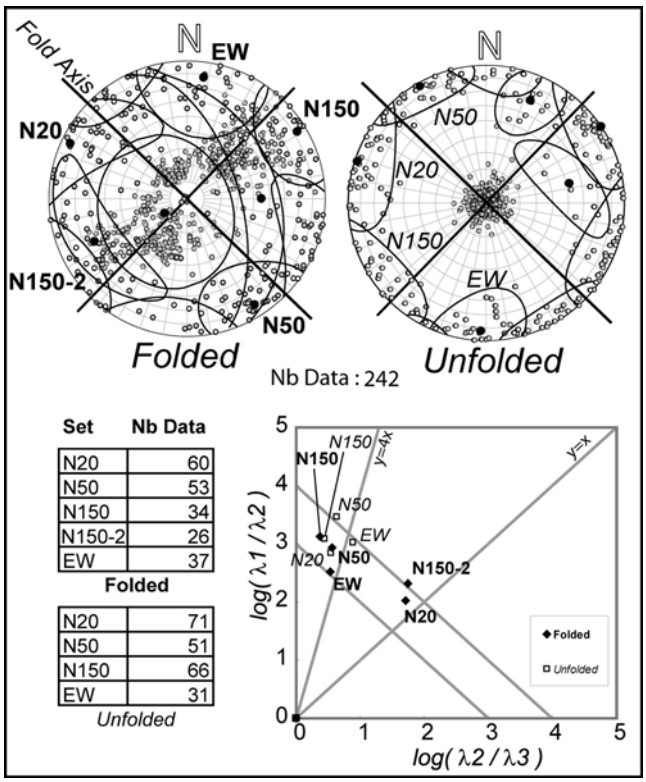

Figure 4. Orientation of the vein sets defined in all the measurement sites. On the stereodiagrams, each pole represents a vein set defined at the scale of a site. These poles are tentatively gathered into regional sets, in both the present position (stereodiagram on the left) and the unfolded position (stereodiagram on the right) using the methodology explained in the text. The larger black dots represent the mean pole of each regional set. The ellipses represent the 95% confidence ellipses of the bivariate normal distribution fitted to each regional set. The table gives the number of data in each set containing a significant number of poles. The names of these sets are plotted on the stereodiagrams and in the bottom right diagram that describes the shape of their orientation matrix [*Woodcock*, 1977]. $\lambda 1$, $\lambda 2$, $\lambda 3$ are the eigen-values of this matrix, along the mean pole axis, intermediate and small axes, respectively. The lines with a slope of -1 correspond to various strength factors $\xi = \log(\lambda 1/\lambda 3)$. The lines passing through the origin correspond to various shape factors γ. The orientations of $\lambda 2$, $\lambda 3$ can by visualized on the stereodiagrams as the two principal axes of the ellipses. The two lines trending at N135 and N45 are respectively the mean fold axis strike and the perpendicular to this strike (the mean fold axes defined as the pole of the large circle fitting all the stratification poles, as the mean of the poles of the large circle fitting stratification poles in each surveyed anticlines, and as the average of fold axis strike measurements made on geological maps are similar).

sets will be presented in order to discuss their chronological relationship with folding.

3.4. Satellite and Aerial Images

[22] In addition to the outcrop scale study where fractures can be directly observed and characterized, satellite (60 × 60 km SPOT 5 scene, HRG instrument, resolution 2.5 m/pixel) and aerial images (from standard 1/50000e plane surveys and helicopter) were used as complementary information to define properly the structural context of the observations made at a smaller scale. Furthermore, this provides the opportunity to compare fracturing at different scales. In our data set, part of the Khaviz and Asmari anticlines in the Dezful Embayment and the SE plunge of the Bangestan anticline in southwestern margin of the Izeh zone were selected for such an analysis based on the quality of the available aerial and outcrop data. The structural maps drawn from the images are used to define the general orientation of major structural lineaments, faults and fracture network. It should be underlined that the objective of the photo interpretation was to define the location and the orientation of the main lineaments and not to precisely map them.

4. Results

4.1. Vein Populations From a Regional Point of View

[23] In a first step, the vein population has been analyzed at the regional scale to study whether regionally consistent sets (called regional sets in the following) can be defined or not. For this analysis, vein sets are defined in each measurement sites as described in 3.3 and then the clustering of these vein sets has been studied in both present and unfolded position (see Figure 12a for a synthetic regional map). The distribution of the poles for each regional set can be quantified using the orientation matrix of each regional set and its representation in an eigen value ratio plot (similar to the popular Flinn diagram, see *Woodcock*, 1977; and examples by *Whitaker and Engelder*, 2005). Because of the fact that most of the measurements were made in sites where bedding dips shallower than 45 degrees, Figure 4 demonstrates that both in the present and unfolded positions the same four major regional sets can be defined: N50°, N150°, N20°, E-W. Two additional sets also shown on Figure 4 are not named and will not be considered hereinafter because they have been too scarcely observed and therefore are statistically unreliable. In the following the relationship between fold geometry and these four main vein sets will be discussed at the scale of single anticlines.

[24] We must remark that these regional sets are dispersed in both positions with strength factors hardly reaching 4 (see Figure 4 for definition). However, the eigen value ratio plot demonstrates that the shape of the distribution of the regional sets is affected by unfolding. In the present position, the N20° regional set is poorly defined. With a shape factor of 1 it is even not statistically significant if one tries to represent it by a monomodal distribution. After unfolding its shape factor changes to a value close to 4.5, indicating than the distribution can be fitted by a bivariate

normal distribution with significant strike dispersion (N-S to N30°). Another major effect of unfolding is to merge the N150° and N150°-2 regional sets (see Figure 4). After unfolding, the regional sets with a E-W and N50° trends are characterized by a strength factor higher than their equivalent in the present position, but the azimuthal dispersion are similar in both positions (shape factor between 4 and 5). It is worth noting that the E-W regional set contains fractures that significantly differ from being perpendicular to bedding. This is consistent with the presence of normal faults with the same trends and suggests that some of the E-W fractures that have been classified as veins from macroscopic description could well be mixed modeI-modeII ("shear") veins.

[25] If we try to relate the orientation of the major regional sets to regional deformation, it is tempting to relate the N150° and the N50° sets to the average strike of fold axis and its perpendicular, respectively, and the N20° set to the orientation of convergence between Arabia and Eurasia, the origin of the E-W set being more enigmatic. It must however be noticed that the N150° regional set trends at 15° clockwise from fold axis. This consistent 15° deviation is preserved even if all the sites are put in a fold reference frame (local fold axis giving the North) instead of a geographic frame and it therefore appears significant. In addition, the dispersion of the data in both the present and unfolded position demonstrates that the vein sets have grown in stress fields heterogeneous at the regional scale [*Whitaker and Engelder*, 2005]. Therefore all these comparisons must be made with great care. This heterogeneity also affects the use of vein set dispersion in folded and unfolded position to discuss the chronology between vein development and folding. Indeed, the overall reduction of shape factor and the increase in strength factor of the regional vein sets suggests that most of the vein sets were created before folding but this observation must be used with caution due to the heterogeneity of their orientation. To tackle these difficulties, the analysis of vein sets at a more local scale is required. In the following sub-sections, we present this analysis in a few key anticlines, keeping the four major vein sets as defined above in the unfolded position (Figure 5).

4.2. Safid and Razi Anticlines

[26] Safid anticline is located in the Izeh zone, in the northern part of the studied area (Figure 2, site 12). Vein orientations were measured in the NE flank through six sites from the base to the top of the Asmari Formation (Figure 6a). It is mainly affected by the N50° and N150° regional sets (Figure 6b). In this anticline, these two sets respectively correspond to fold-parallel and fold-perpendicular veins. Some of them show well preserved fractographic structures, and they form very regular networks made by rectilinear fractures with constant spacing (Figure 5a), suggesting that they were both created as systematic joint sets.

[27] The Razi anticline, located in the southeast corner of the studied area, shows a similar vein population (Figure 7a). However, along the surveyed section a third set trending N10° to N30° can be observed (N20° regional set). It is noteworthy that this anticline is a gentle fold with bedding dip in the exposed flanks poorly reaching 10°. Despite this weak deformation intensity, vein density is high on the outcrop (Figure 7b) when qualitatively compared to the other outcrops described in this paper.

[28] In both anticlines, no direct relative chronology between vein sets was observed. Unfortunately, the trend of the veins with respect to fold axis in Safid anticline and the very low bedding dips in Razi anticline do not allow testing any hypothesis concerning these chronologies using unfolding.

4.3. Asmari Anticline

[29] The Asmari anticline (Figure 2, site 1) is located toward the northwest of the Dezful Embayment and west of the IZHF. We measured vein orientations in 13 sites selected in the south-western flank, the crest, the north-eastern flank and the south-western plunge of this anticline. These veins are normal or slightly inclined with respect to bedding planes. On the basis of their orientations (Figure 8a), these veins have been gathered into the N50°, N150° and N20° regional sets. The first two are similar to sets observed in Kuh'e Safid and Razi, trending respectively sub-perpendicular and subparallel to the fold axis that was determined from bedding plane measurements and mapping on aerial photo. One should however notice that the N150° set trends at 10° to 20° clockwise from the fold axis as noticed on the regional analysis of the orientation data. The lineament directions observed on aerial photos (Figure 8c) also show similar trends except that the one striking close to the fold axis is rotated by 10° from this axis.

[30] From the orientation map (Figure 8a), it appears that the N150° vein set is best expressed in the southwest flank of the anticline. This can be due either to outcropping condition (the valley in which the measurements was carried out is perpendicular to this set), or a real increase in the vein density for this set. Such a density increase is weakly observed on the lineament map. The N20° vein set (especially the N-S subset) is more represented in the south-eastern part of the Asmari anticline as the large scale lineament with this strike observed on aerial photos and can be correlated with the presence of dextral N-S trending faults as previously mentioned by *McQuillan* [1973].

[31] Some of the sites described directly on outcrops were also surveyed using a helicopter. On the crest of the anticline toward its south-eastern nose helicopter photos provide constraints on the chronology among these vein sets (Figures 9a and 9b). In this area, structural dip is gentle, nearly horizontal and the trend of the fold axis is about N130°. Figure 9b shows that veins belonging to the N50° regional set form a very systematic pattern without any directional perturbation. At the same location, longitudinal lineaments are organized in swarms made of veins belonging to the N150° regional set. As some of these veins abut on N50° veins, this suggests that the latter developed first. Such a chronology is further compatible with the fact that the N50° set appears as very regular pattern. Finally, the N20° regional vein set corresponds to relatively short rectilinear veins frequently abutting on the N50° and N150° veins. In addition, some of these veins are branching on N150° veins

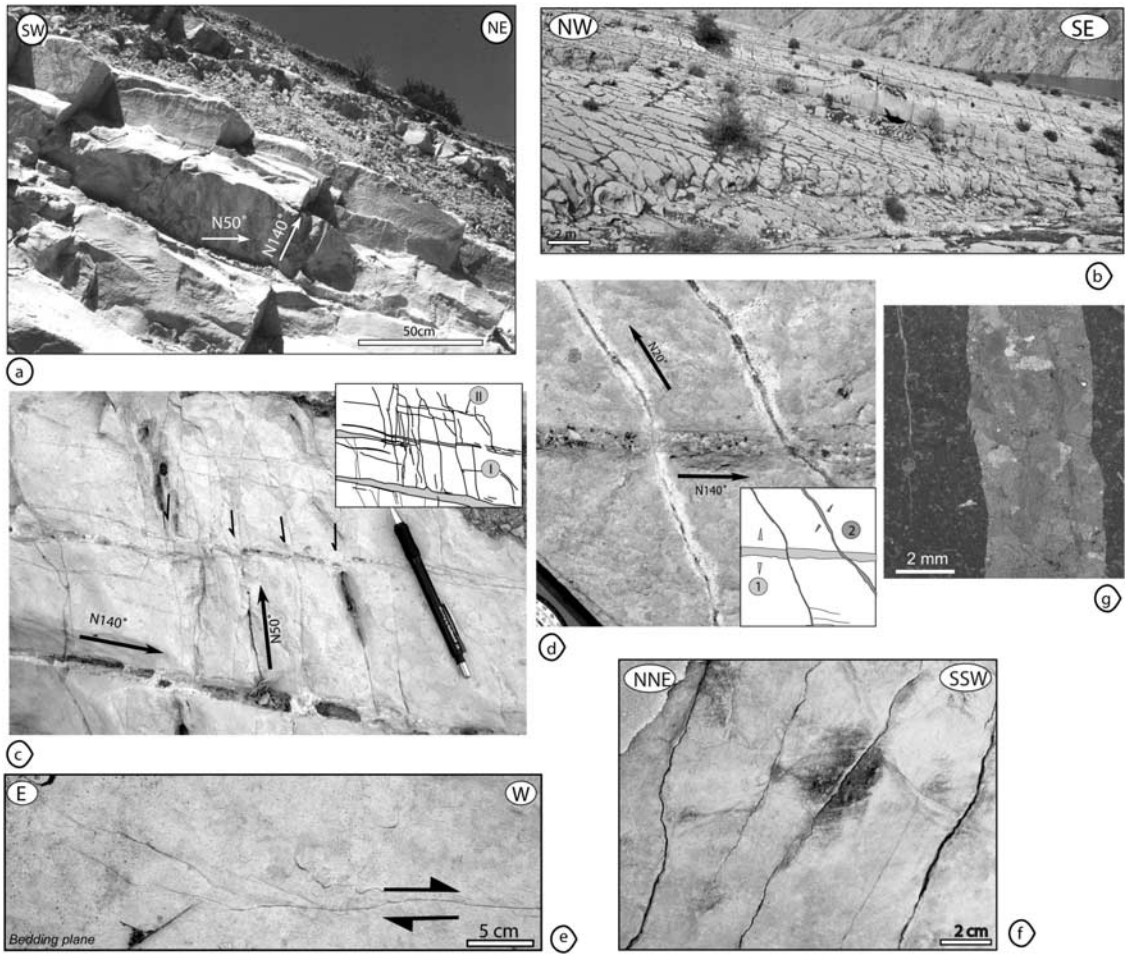

Figure 5. Most frequent tectonic microstructures observed on the outcrops. (a) Veins with remaining plumose structures on the walls (cements have been weathered on exposed walls) suggesting that part of the veins initiated as joints (Safid anticline). (b) Typical general view of a vein network (Bangestan anticline). (c) and (d) details of the veins shown in b) showing typical examples of sheared veins parallel to the regional N20° and N50° vein sets. The presence of both veins and sheared veins along these directions suggests that joints or veins developed first and were later on reactivated in shear with a bit of opening by a NNE shortening. This reactivation postdates the opening of the N140°-150° veins that are displaced by shearing. (e) Example of horsetail structure showing that at least part of the movement along some veins corresponds to shearing (Dil anticline). (f) Example of tectonic stylolite (cross section view); (g) Example of thin section cut in a vein observed in natural light (Khaviz anticline).

forming dextral horsetail structures (Figure 9a). These observations demonstrate that at this location the N20° set postdates the N50° and N150° sets and that the later was reactivated during the growth of N20° veins. Finally, concerning chronology, it is worth mentioning that the strike dispersion of the N150° veins is significantly reduced in the various sites after unfolding (Figure 8c). The same reduction, though less significant, can be observed for the N20° set. These observations suggest that at least the N50° and N150° sets were created before folding in accordance with the bed-perpendicular attitude of the veins belonging to these sets.

[32] In conclusion, three main episodes of vein development are identified in the Asmari anticline: first, formation of a N50° systematic vein set, followed by the development of a N150° set, almost parallel to the fold axis. Finally, a late N20° regional set developed in the vicinity of N-S dextral strike-slip faults, with a strong control by the occurrence of the pre-existing sets.

4.4. Khaviz Anticline

[33] The Khaviz anticline is located between IZHF and KMF (Figure 2, site 6). This anticline has a rectilinear geometry with a general structural trend of about 115° and average dips in the flanks in the range of 30°. The vein orientations have been measured in ten sites around the south-eastern nose of this anticline (Figure 10). Four vein sets are observed in these sites (Figure 10a): N150° ± 10°;

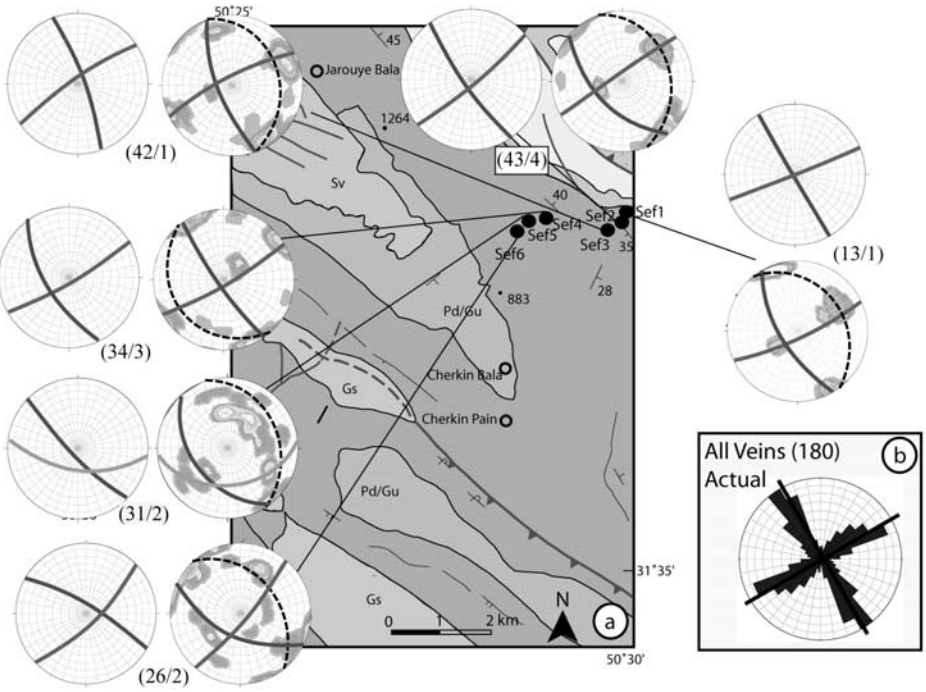

Figure 6. (a) Vein set orientations in the Safid anticline. Stereodiagrams: Schmidt lower hemisphere; black dashed semi-circle is bedding plane. Both measured data sets (with fracture density diagram at the background) and back-tilted (unfolded) data sets (without density diagram at the background) are shown. Number of data veins/bedding in parentheses. (b) Rose diagram of all the veins (number of data given in parentheses).

N50°, N10° ± 10°; N80° ± 10°. The N150° ± 10° is clearly the most frequently sampled set (Figure 10c), followed by the N80° ± 10°. As in Asmari anticline, the former is trending at 10° clockwise from the fold axis that is locally rotated to N130° in the southeastern termination. Large scale lineaments were well identified in the northwestern part of the anticline due to the availability of a Spot V image in this area (Figure 10b). On the basis of their consistent trends, these lineaments (Figure 10c) can be classified into sets similar to vein sets except that the N150° trend is lacking, being replaced by a N110°–120° set parallel to the anticline axis. The N110°–N120° set corresponds to normal faults observed in the field that have been interpreted so far as due to crestal collapse normal faults [*McQuillan*, 1973; *Wennberg et al.*, 2007]. Therefore both the vein sets and the lineament population are very similar to those described in

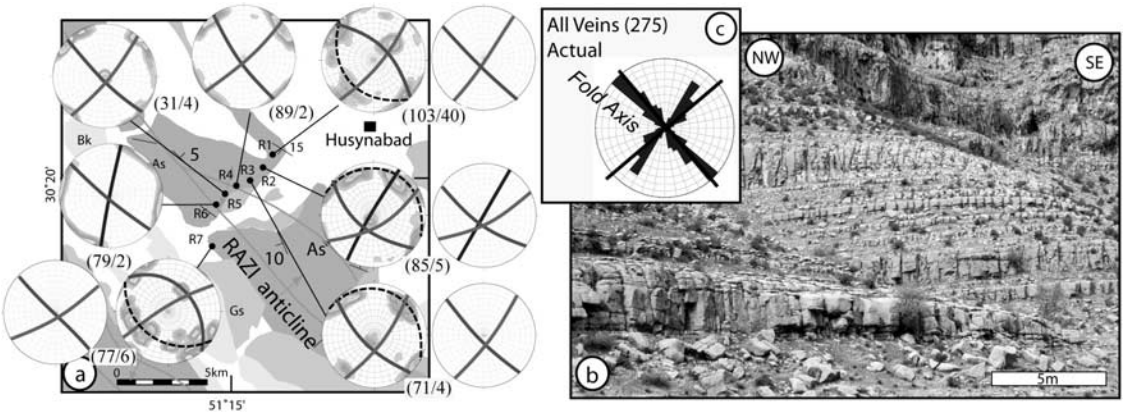

Figure 7. (a) Vein set orientations in the Razi anticline (Stereodiagrams: same key as in Figure 6a). Sites R1, R2, and R5 with the fracture set parallel to the fold axis are located in a small flank syncline. (b) Fracturing in subhorizontal beds of the Razi anticline. (c) Rose diagram of all the veins (number of data given in parentheses).

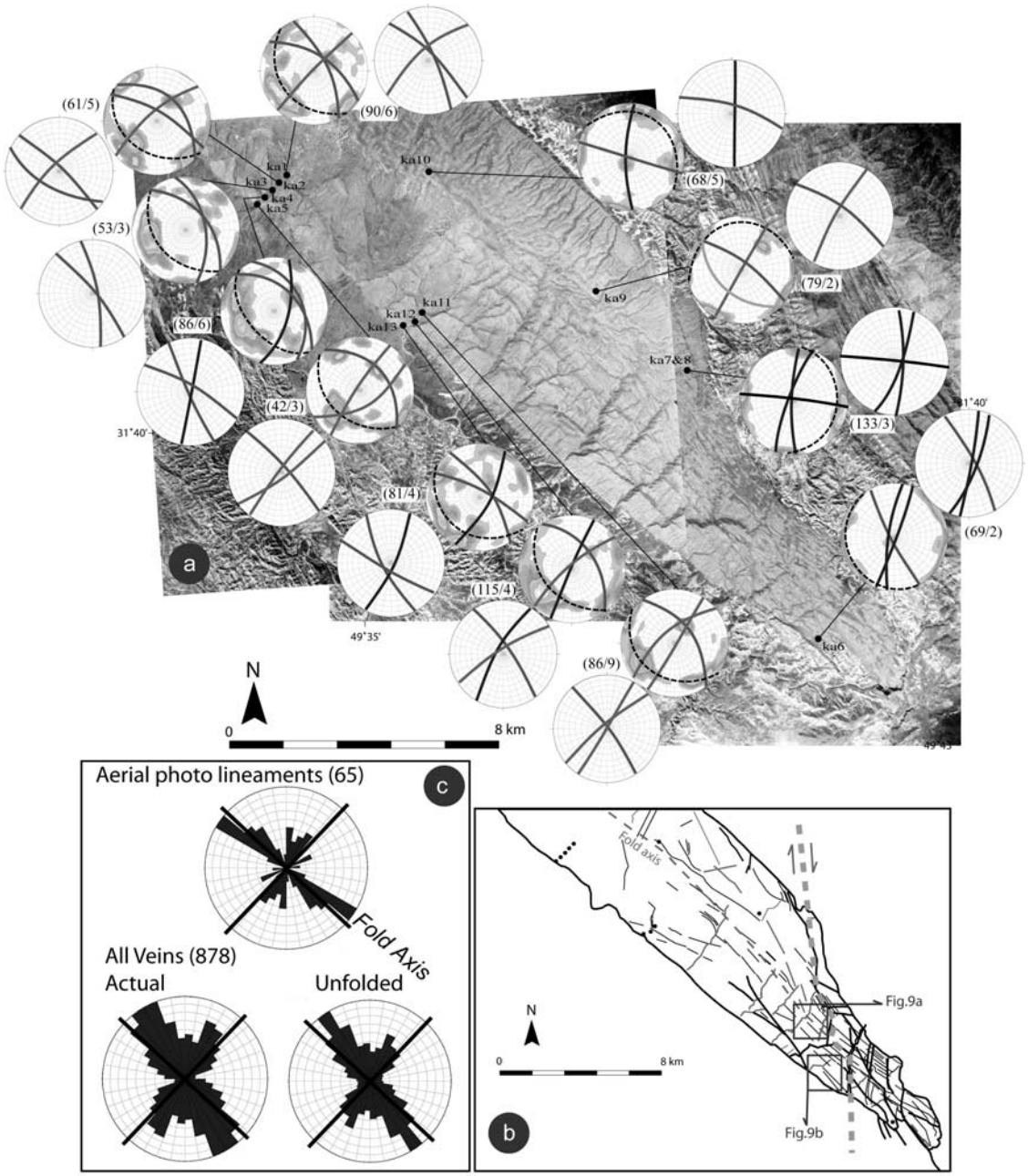

Figure 8. (a) Vein set orientations in the SE part of the Asmari anticline (Stereodiagrams: same key as in Figure 6a) as measured in 13 sites. (b): Interpretation of main lineaments. Note the probable influence of a right-lateral N-S trending basement fault beneath the SE part of the fold. (c): Rose diagram of the veins sets in present and unfolded position and lineaments strike (number of data in parentheses).

the Asmari anticline located 150 kilometers away and although the axis of the latter is trending N130°–N140° instead of N115° to very locally N130°. The main difference between the two anticlines is that the N20° and N50° regional sets where dominantly sampled in Asmari anticline whereas the E-W set appears much more frequently sampled in the Khaviz anticline. This set is very well developed in the southern part of the anticline termination, where in addition numerous small scale normal faults parallel to this set and with a variable amount of strike-slip movement were observed.

[34] The chronology between the vein sets can be constrained by the geometrical relationships between veins and the history of fillings (e.g., Figure 5g). Two main types of fillings are observed: the first one is made by clean calcite, while the second corresponds to a brown calcite enriched in Fe. The N20° veins are mostly filled by clean calcite. The E-W veins have been filled with two types of calcite: (i) the

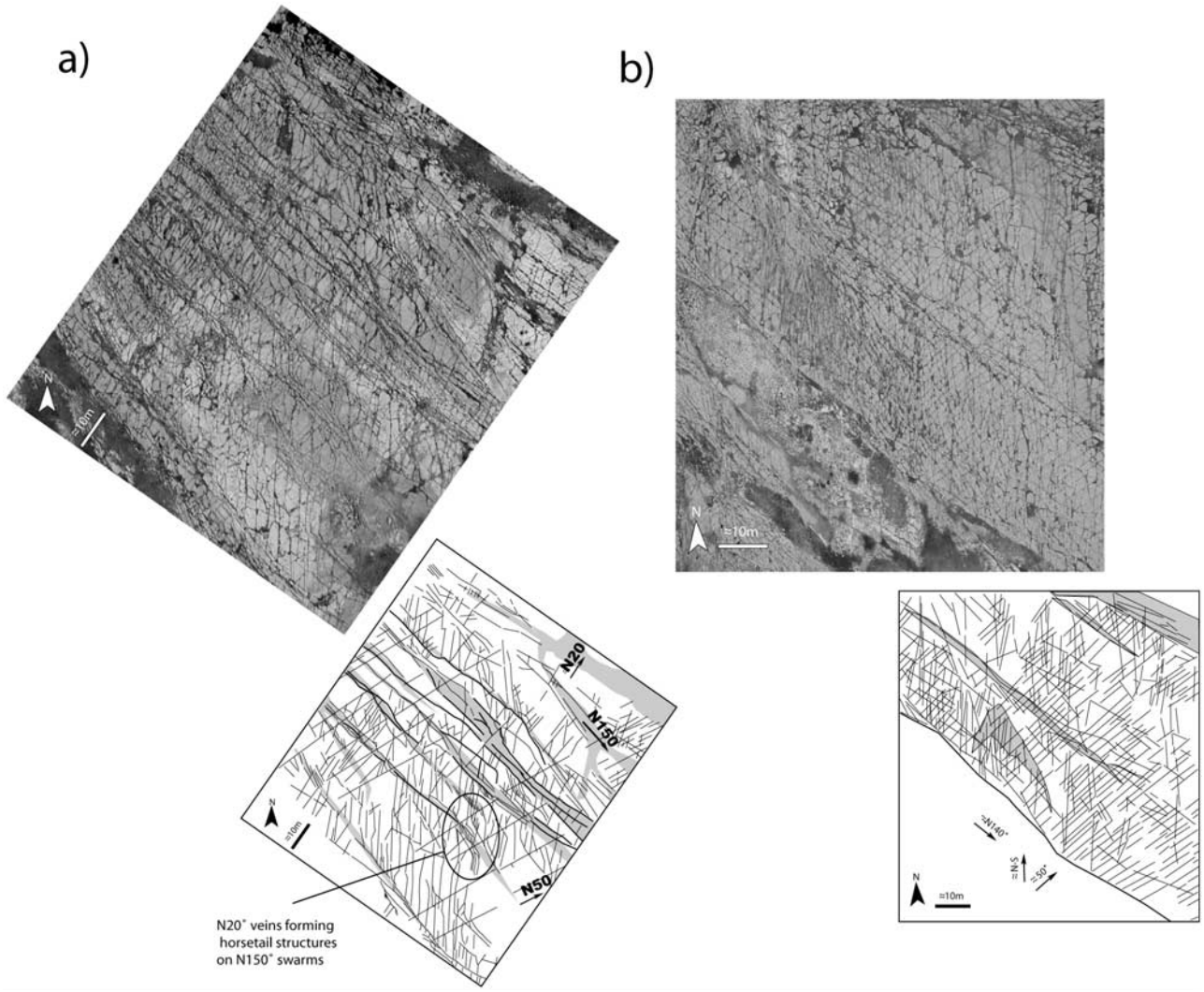

Figure 9. Main vein sets observed on the southern nose of the Asmari anticline (location on Figure 8b). (a) The regular vein set with an azimuth close to N50° appears as the first set; N130° trending veins form a series of clusters almost parallel to the fold axis; N20°–30° and also N-S vein sets abut onto the previous sets. (b) Regular N50°, N-S and N140°–150° vein sets.

clean calcite similar to the one filling the N20° veins is observed at the margin of the veins, (ii) the brown calcite occupies the center of these fractures, showing that the brown calcite postdates the clean one. N150° veins are filled exclusively by the brown calcite. As an example repeatedly observed in the southern part of the nose, Figure 11 demonstrates that N20° veins formed first, followed by E-W veins that frequently abut on them. Finally N140°–150° were created, filled by the brown calcite (Figure 11). In addition, dextral strike-slip movements (not shown on the Figure 11) are frequently observed along E-W fractures where they are widely open and filled by the brown calcite.

[35] To summarize, the Khaviz anticline shows the successive development of N20°, E-W, and N150° vein sets. The fourth regional set, N50°, is observed, but cannot be tied to the others in term of chronology.

4.5. Supplementary Fracture Data

[36] As shown in Figure 12, vein sets were investigated in other anticlines of the Dezful Embayment. Some of the important observations made in these anticlines are summarized below.

[37] The Bangestan anticline is one of the giant folds in the Izeh zone. The SE nose of this anticline is affected by vein sets very similar to those observed in the anticlines already described: N150°, N50°, N20°. Similar trends are also observed at large scale as lineaments on the SPOT 5 image (Figure 13). Though the chronology between the formation of N140° and N20° veins is not clear, there is no doubt that sinistral shearing along N50° veins postdates the large opening of N140° ones (Figure 5d). This demonstrates that, as in Asmari and Khaviz anticline, a NNE-oriented

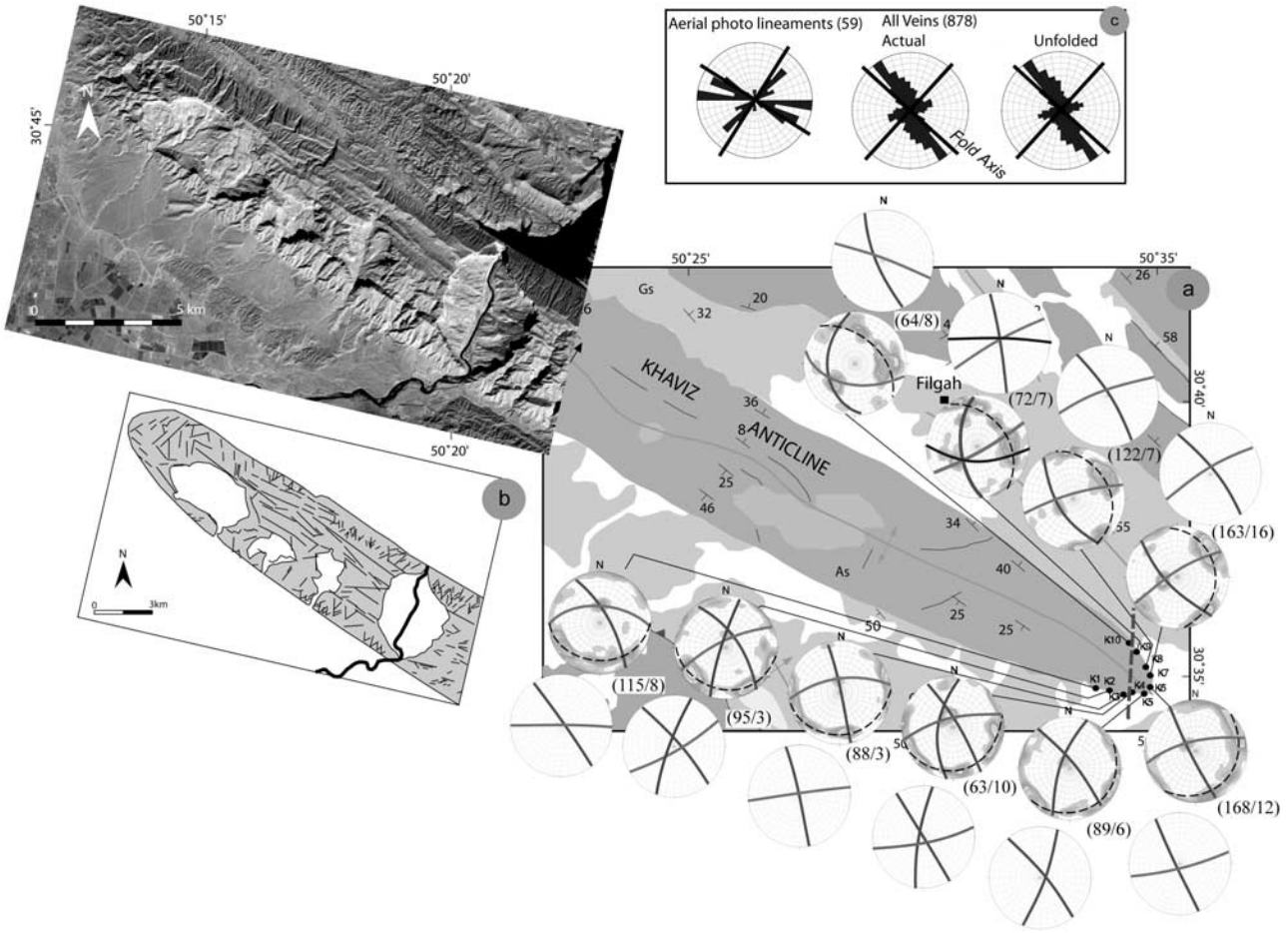

Figure 10. (a) Vein orientations in the SE termination of the Khaviz anticline (Stereodiagrams: same key as in Figure 6a). The prominent vein set, striking N150°, is persistent around the anticline termination. The prominent N–S vein trend observed in the sites K3, K4, K9, and K10, is likely the effect of a N-S trending fault zone, indicated by a thick dashed line. (b) Main lineaments interpreted form a SPOT V satellite image on the western part of the Khaviz anticline. (c) Rose diagram of the veins sets in present and unfolded position and lineaments strike (number of data in parentheses).

compression was prevailing after the opening of the N150° veins.

[38] The Dil anticline (Figure 12, site 4) provides interesting observations to analyze the relationship between folding and vein development because its axis turns from nearly E-W toward SSE from West to East. This change can be related to the influence of the nearly N-S trending Kharg-Mish basement fault (KMF) and its amount suggests that the fold formed with this primary bend instead of having been secondarily bent by shearing due to strike-slip motion. On Figure 12, two sites are presented in the northern flank of this anticline where the average structural dip is close to 40° with a strike changing from N120° to N150°. This figure shows that whatever the dip, the vein population is made of two major sets perpendicular to bedding: a nearly E-W striking one (N90° to N70°) and a sub-meridian one (N10° to N20°). This suggests that these two vein sets were created independently from folding. Evidence of shear movements postdating the opening of these veins demonstrates that they have subsequently been reactivated during folding.

[39] Finally, the analysis of Figure 12a demonstrates that anticlines located at the vicinity of the Izeh-Hendijan fault (IZHF) are dominated by N20° and E-W veins sets. This is the case for Shur, Chalkhushk, Sulak, and Lappeh anticlines. Interestingly, these sets remain dominant in these anticlines whatever the local trend of the fold axis. While the N20° vein set is oblique to local bedding azimuth in Chalkhushk and Shur anticlines (Figure 12, sites 13&3), it is perpendicular to local fold axis in the Quirak and Sulak anticlines (Figure 12, sites 10&14). It is noteworthy that similar vein populations are observed in the NW nose of the Khami anticline (Figure 12, site 5a&b) located close to the KMF.

[40] These supplementary observations demonstrate that a large part of the vein population appears to be independent from fold geometry, being partly controlled by the location

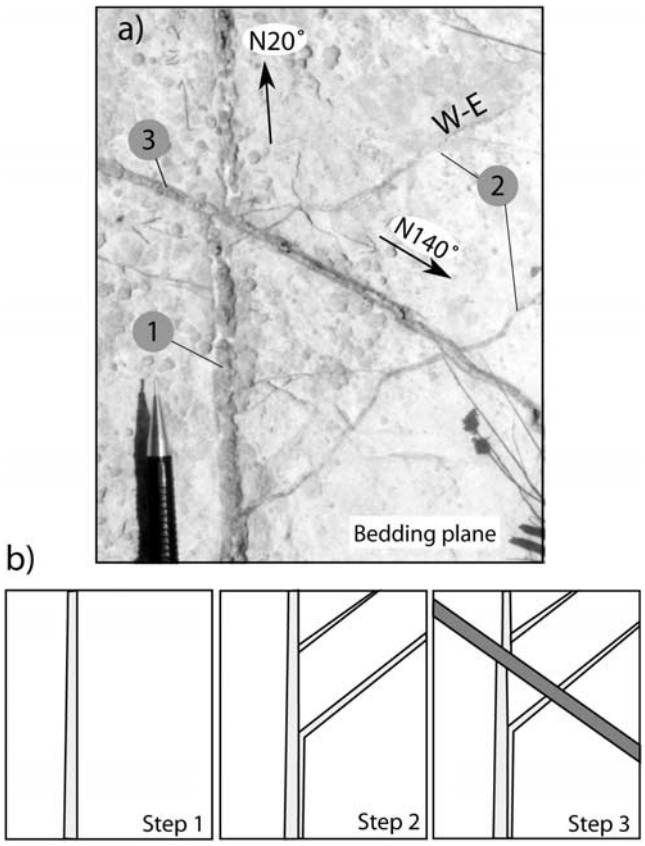

Figure 11. Chronology between the N20°, E–W and N150° veins in the SE nose of the Khaviz anticline. (a) Outcrop photo, (b) sketch of the vein evolution taking into account crosscutting relationship between veins, geometry and nature of the cements. In light grey clean calcite filling, in dark grey, calcite enriched in Fe, brown color on the outcrop. See text for details.

of the sites with respect to underlying basement faults (Figures 12a and 12b).

5. Interpretation of Results and Discussion

[41] Fold-related fracture models [*Stearns and Friedman*, 1972; *Price and Cosgrove*, 1990] are widely used by structural geologists to explain fracture populations in a typical fold. However, the relative chronology of different sets and their reactivation, as well as the possible effect of inherited fractures on fold geometry are sometimes overwhelmed in most of these models, and only few models attempt at including prefolding joints in the kinematic history [e.g., *Bergbauer and Pollard*, 2004]. The fold/fracture relationships involved in most of these models are in poor agreement with observations reported above: (i) N20° vein sets are consistently observed in the eastern part of the Asmari anticline, (ii) N50° vein sets predates all the other sets whatever the location within fold, (iii) the N150° set, sub-parallel to fold axis is observed in the flanks far from the crest of the anticlines, (iv) in Kuh-e Khaviz this set is clearly oblique to the fold axis. In Kuh-e Dil, the orientation of the various sets appears independent of the orientation of the characteristic geometrical elements of the fold. In addition, a clear chronology between the various vein sets could be identified. Therefore the progressive deformation of the Asmari Formation since the onset of Arabia-Eurasia collision should be taken into account to explain the observed vein populations.

[42] Furthermore, the geometry of some folds is more complicated than the general trend of the Zagros fold belt. Some examples of this complexity are provided by the axial rotation of Mongasht, Bangestan, and Dil anticlines in the studied area (Figure 2). These local rotations of fold axis are located above well-known basement structures [*Motiei*, 1993]: when they are small, these rotations can be due to strike-slip movement at depth along these structures as suggested by the seismicity, or to the changes in the depth of decollement level across these lineaments [*Sherkati et al.*, 2006], or even to basement topography. Unfortunately, the geometry of these structures is still insufficiently constrained to define the relative influence of these mechanisms. However, seismicity data [*Jackson*, 1987; *Berberian*, 1995] and the detailed analysis of the thickness of Tertiary formations demonstrate that these basement structures were active since the deposition of Asmari [*Abdollahie et al.*, 2006]. This is in agreement with the fact that specific vein sets are found mainly in their vicinity.

[43] In order to explain the chronology of the vein sets described in this paper together with the role of basement faults, we propose a conceptual model of vein development in the Central Zagros (Figure 14) based on our field observations. This model includes the following major steps: (i) development of joint/vein sets related to the onset of collisional stress build-up in the Zagros sedimentary cover, (ii) development of vein sets related to extension caused by large-wavelength drape-folds above compressionally reactivated basement faults, (iii) reactivation of the early vein sets and development of classical fold-related fractures during the main Mio-Pliocene episode of folding.

5.1. Prefolding Vein Populations in the Central Zagros

[44] Hereinafter, the general terms of fold, folding and fold-related veins will be used for the final orogenic event, leading to the development of folds and thrusts in the Zagros belt during Miocene-Pliocene times [*Stoecklin*, 1968; *Falcon*, 1974; *Colman-Sadd*, 1978; *Berberian and King*, 1981; *Motiei*, 1993; *Alavi*, 1994; *Sherkati et al.*, 2006], together with the general involvement of the basement in shortening. To this respect, veins that possibly developed early in association with large wavelength forced-folds or flexures related to reactivation of N-S and N140°-trending basement features before the main Mio-Pliocene shortening event will be referred to as prefolding veins. In order to give a simpler overview of prefolding vein sets and the specific occurrence of some of them in the vicinity of basement faults, dominant vein sets have been extracted from the total set of Figure 12a and reported in Figure 12b in their unfolded attitude together with the main basement trends.

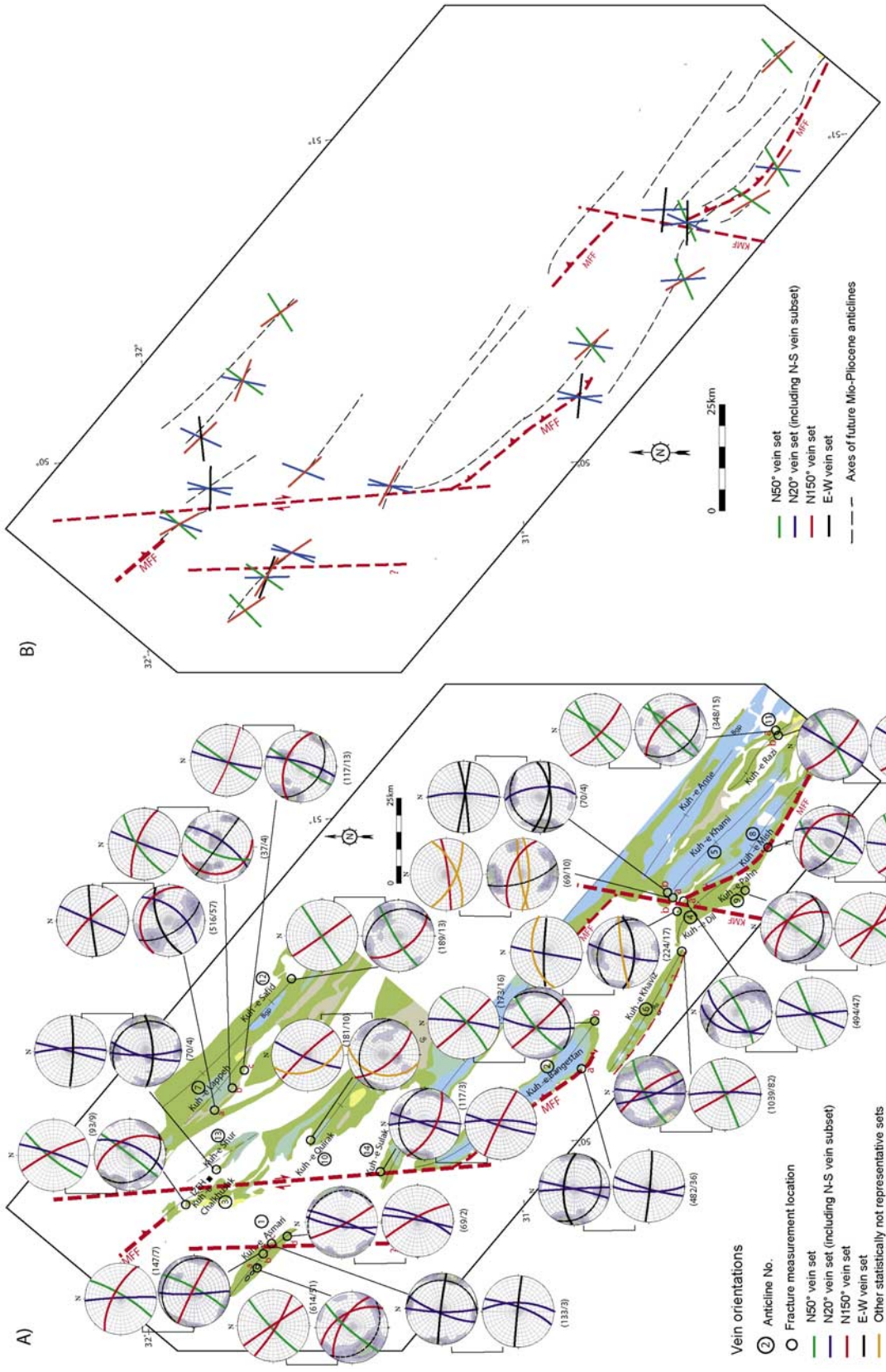

Figure 12. (a) Map of the vein sets defined in all studied sites. (Stereodiagrams: same key as in Figure 6a). (b) Sketch of the main prefolding vein sets in each site defined from Figure 12a together with the large scale tectonic structures (red dashed line: transverse lineaments, with triangle: main thrusts, grey dashed lines: future anticline axes). Note the almost specific occurrence of N20° and E-W vein sets in the vicinity of N-S basement faults.

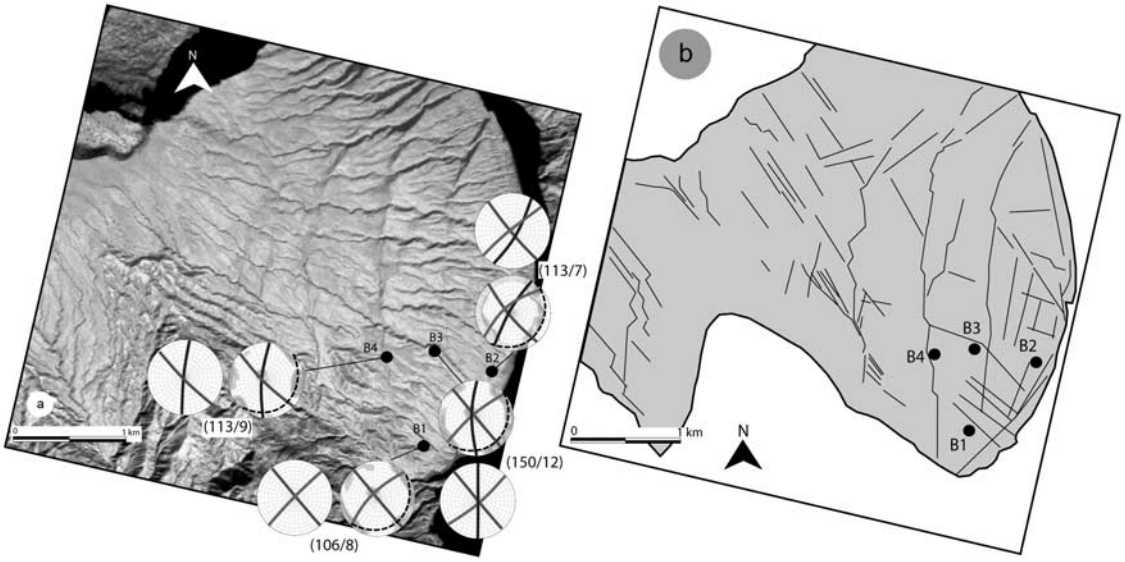

Figure 13. (a) Fracture orientations and (b) major lineaments in the SE nose of the Bangestan anticline (Stereodiagrams: same key as in Figure 6b). Note that the trend of the prominent vein set measured in each site is compatible with the trend of the main lineaments (faults or high density fracture zones) observed close to the measurement site.

5.1.1. N50° Prefolding Joints/Veins Related to the Onset of Stress Build-up

[45] Based on our observations, the N50° vein set appears to have developed first (Figure 14a). The attitude of these veins with respect to bedding in fold flanks indicates that they predate folding and should be interpreted in their unfolded attitude. The strike of this set is likely related to the orientation of the regional stress field. It is therefore not necessarily perpendicular to present-day fold axis or to the local bedding strike (e.g., in Asmari, Khaviz, and Bangestan anticlines) and may depend on how efficiently the N-S convergence between Arabia and Eurasia has been partitioned between the thrust belt and strike-slip at the rear. Development of this set could be synchronous with the formation of the tectonic stylolites whose peaks generally indicate the same direction of shortening. We propose that this vein- stylolite association marks the earliest stress build-up in the cover of the Zagros in response to the orogenic far-field stress as it is frequently reported in the foreland of thrust-belts. Defining the absolute age of this earliest set could be a key point toward the determination of the timing of the onset of deformation within the Zagros basin. It presumably predated shortly reactivation of basement faults as proposed in the conceptual model and deformation scenario. If the timing of the early basement fault reactivation can be improved [*Abdollahie et al.*, 2006], it may lead to definition of the absolute age of the onset of deformation.

5.1.2. N150° and N20° Prefolding Veins Related to Early Reactivation of NW-SE and N-S Trending Basement Faults and Related Flexure/Forced Folding

[46] N150° veins: The strike of this main set is more or less parallel to the overall mean trend of fold axes, so it mimics those of fold-related fractures which are parallel with the fold axis and which developed in response to local outer rim extension. However, in detail, these veins are frequently trending at 10° to 20° clockwise from the fold axis (Figure 4 and Figure 12a). In addition, in the Lappeh anticline, in spite of important variations in structural dip in measurement sites, these apparent axial veins are rarely seen whereas they are frequent in other anticlines within the same structural position. In the Razi anticline (Figure 7) which displays a much more flat-lying bedding attitude compared to the other studied anticlines, this set is prominent. In agreement with *McQuillan* [1973], concerning the lack of relation between deformation intensity and fracturing within Asmari Formation, we suggest that, at least for this vein set, local bed curvature related to folding seems not to have played an important role in their initiation. There are two points to this regard which argue against a simple fold-related nature for this set, even though a late, syn-folding reopening of these early fractures is likely. In the Razi anticline, the measured stations, R1 and R2, are located in a gentle syncline, where the N150° set is observed. In these stations, outer rim extension is unlikely in the concave-upward part of the syncline, so that this extension might rather have been caused by a flexure/drape fold with a wavelength larger than the one observed today. Another evidence of prefolding development of N150° set is provided by vein distribution around the terminations (periclinals) of the folds. If one supposes that fold-related joints usually propagate normal to the principal minimum stress, their trend should change around the periclinal regions of the folds [whatever the chosen model, *Stearns and Friedman*, 1972; *Gholipour*, 1998]. It means that their trend should change with respect to the mean fold-axis or local bedding trend variations. Periclinal regions of the folds in the studied area, however, do not show such an agree-

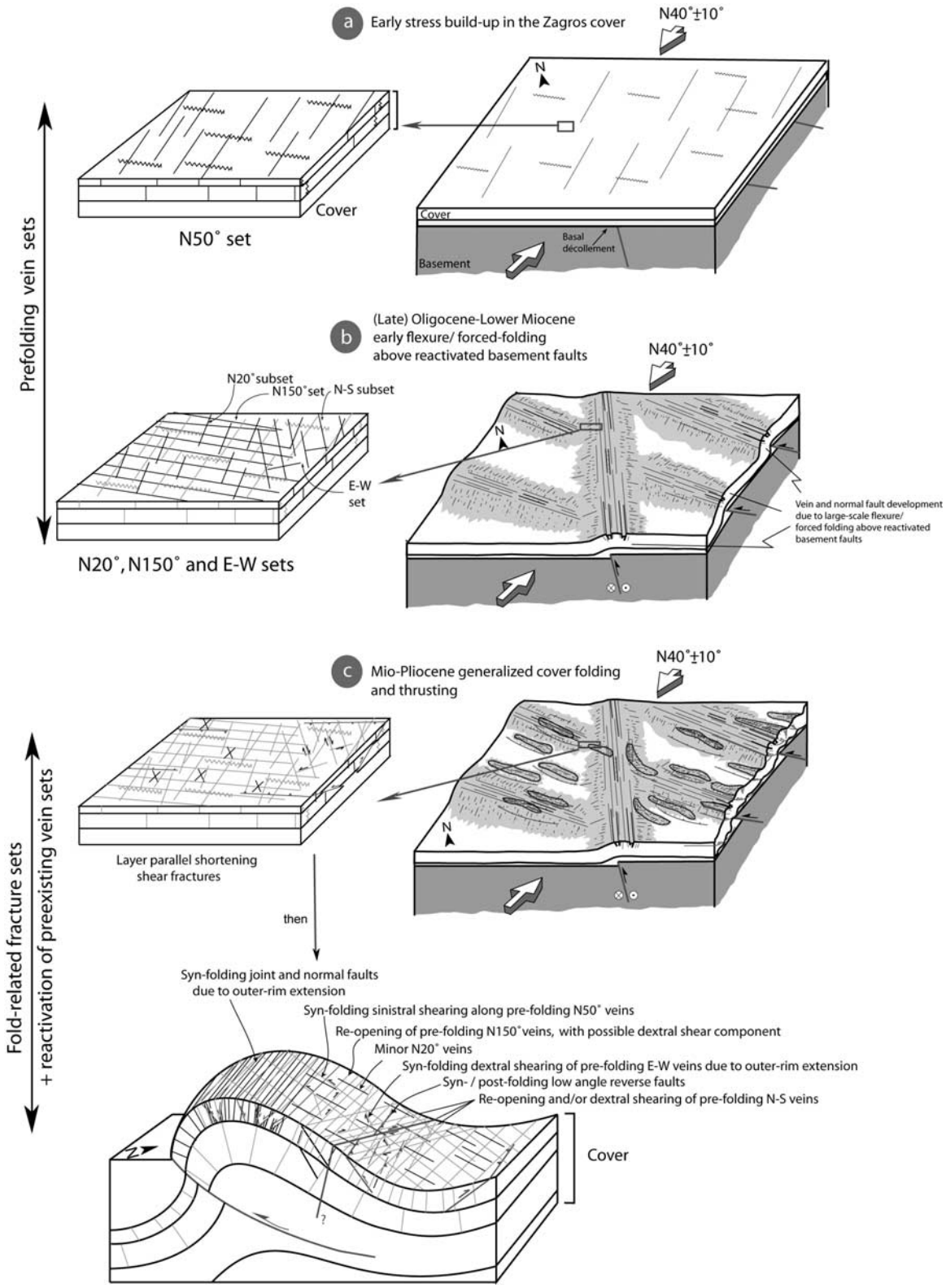

Figure 14. Conceptual model for vein development within the Asmari Formation in the central Zagros folded-belt (see text for more details), putting emphasis on prefolding, regional veins development (stages a and b), followed by generalized folding of the Zagros cover and reactivation of early vein sets (stage c).

ment between veins and local bedding trend. In the SE nose of the Bangestan anticline, the N150° veins form the prominent set but the local bedding azimut is not parallel with this vein set (Figure 12, site 2b). Many long valleys on the SE plunge of the Bangestan anticline have developed parallel to this prominent vein direction. Accordingly, lineament directions parallel to this vein set on the satellite image on the nose of the Bangestan anticline do not follow bedding attitude changes (Figure 13). Almost the same situation is observed on the SE nose of the Khaviz anticline, where N150° trending veins are again a prominent vein set. In this anticline, the model of fold-related fracture population cannot explain the relative orientation stability of the N150° veins.

[47] From the observations and examples mentioned above, a model of fold-related veins therefore does not apply to the N150° set. One explanation would have been to form the N150° vein set after the formation of the fold. Unfortunately due to the heterogeneity of vein orientation (Figure 4) fold test are poorly conclusive. The simplest explanation consistent with the fact that these veins are observed as being cut during the reactivation of other sets (Figure 14) is that they predate folding. We therefore suggest that the N150° vein set initially formed in response to a local extension caused by large-scale flexure/drape folds above reactivated NW-SE trending basement faults (i.e., the HZF, MFF, DEF and ZFF) (Figure 14b). In response to the onset of collisional stress build-up, these basement faults, which strike nearly parallel to the general axial trend of the Zagros folded belt, likely underwent a nearly dip-slip reverse component of motion [*Ahmadhadi et al.*, 2007]. Such early basement fault movement predating Mio-Pliocene cover folding has been recently documented in the studied area [*Abdollahie et al.*, 2006] but also in the neighboring Fars area [*Mouthereau et al.*, 2006; *Mouthereau et al.*, 2007]. On the basis of evidence of facies changes and thickness variations of Oligocene to Miocene formations, *Ahmadhadi et al.* [2007] proposed that large-scale flexure and/or forced folding caused by compressionally reactivated deep-seated basement faults in the Central Zagros have affected the Zagros foreland basin as soon as the late Oligocene- lower Miocene, especially during deposition of the Asmari Formation. The resulting large-scale flexure/forced-folds [*Cosgrove and Ameen*, 2000] may have caused local extension leading to development of N150° veins and even associated normal faults (e.g., Khaviz and Sulak anticlines). The role of the basement faults, either in form of inverted pre-existing normal faults [*Jackson*, 1980; *Hessami et al.*, 2001] or high-angle reverse faults [*Falcon*, 1974; *Berberian*, 1995], should therefore not be overwhelmed in the initiation of veins and other fractures within sedimentary strata of the Zagros, but also of other fold-thrust belts. Even, thrust faulting and folding within the sedimentary cover are often triggered and controlled by basement faults [e.g., *Lacombe and Mouthereau*, 2002]. With such model in mind, the obliquity between the N150° set and the fold axis could be either related a small component of dextral strike-slip on N140° trending basement faults (this trend controlling more firmly the fold geometry than fracturing) or to an obliquity between the direction of the basement faults that control the orientation of the early drape folds with respect to later folds related to Mio-Pliocene shortening.

[48] N20° veins: Locally, N20° veins appear to postdate the other vein sets (e.g., Asmari anticline). Again, this set does not follow fold geometry and it has been mostly identified in the vicinity of N-S trending basement faults (e.g., IZHF and KMF, Figure 12).

[49] In detail, the so-called N20° set comprises a N-S subset and a N20°–30° subset that were hardly separated in the global statistics but could be identified in some sites. In Dil and Mish anticlines (Figure 12, sites 4&8) the N-S subset has been recognized as a systematic vein set with no simple geometrical relationship with fold shape. In the Asmari anticline it has been observed next to a N-S trending faults in the eastern part of the fold (Figure 8). Since early transpressional (dextral) reactivation of the N-S trending basement faults could have occurred more or less contemporaneously with the reactivation of the N140° basement faults parallel to the Zagros trend, in Oligo-lower Miocene times [*Abdollahie et al.*, 2006; *Ahmadhadi et al.*, 2007], we propose that the N-S vein subset has a direct relation with underlying N-S basement faults and may have developed with a nearly similar flexure/forced-folding mechanism than, and synchronously with, N150° veins (Figure 14b); the N20°–30° subset likely reflects a slight change of the regional compressional trend (evolving from N050° to N020°–030°, and therefore N040 ± 10° on average, Figure 14), possibly in the vicinity of N-S basement faults reactivated as right-lateral strike-slip faults. This could explain some of the conflicting chronological relationships observed between the 150° and the N20° sets (the N20° vein set appears to predate the N150° vein set in the Kuh'e Khaviz outcrop, Figure 11, but usually postdates the 150° vein set in Kuh-e-Asmari).

5.1.3. E-W Vein Set

[50] In the studied area, a minor E-W vein set trending oblique to the fold axis has been observed, mainly in places where an underlying N-S trending fault is encountered (e.g., Dil, Khami, and Sulak anticlines, Figures 12a and 12b) and where the N20° set (especially the N-S subset) is well developed. There is little evidence for any regional or local E-W trending compression or N-S trending extension; but the close spatial association between this set and the N20° set suggests that they are both controlled by the N-S regional trends.

[51] To summarize, we propose that the N150° vein set which clearly predates cover folding likely developed in response to large-scale flexures/forced-folding above reactivated NW-SE trending basement faults (e.g., MFF, ZFF) which could have induced extension within the uppermost part of the sedimentary cover (e.g., the Asmari limestones). This early reactivation of NW-SE basement faults as soon as the late Oligocene-lower Miocene is supported by thickness variations and facies changes documented in the Zagros foreland basin at that time [*Ahmadhadi et al.*, 2007]. In a similar way, the observed N20° vein set (e.g., Khaviz anticline) and the E-W set, and the location of measurement sites containing these vein groups near underlying N-S

trending basement faults (e.g., IZHF and KMF, Figure 12b) suggest that these sets could have also initiated quite early (i.e., before Mio-Pliocene cover folding), in relation to the transpressional (dextral) reactivation of the N-S basement faults, and presumably coevally with the compressional reactivation of the NW-SE trending basement faults.

5.2. Fold-Related Fractures in the Central Zagros

[52] In addition to vein sets described above, fractures unambiguously related to the main phase of Mio-Pliocene cover folding could also been observed. They are mostly low-angle shear fractures, reverse faults, thrusts and duplexes, which are normally seen near synclines axes. From a geometrical point of view, most of these structures have formed consistently with the N040° ± 10° directed compression responsible for the main deformation event in the Zagros area. The reactivation of the preexisting veins likely happened in this stage as well. As examples, we can mention (i) dextral shearing along N-S veins, (ii) sinistral and dextral shearing along E-W veins, due to regional compression then local outer arc extension, respectively, and also (iii) sinistral shearing along N50° veins (Figure 5b). This shearing was even observed along NW-SE trending fracture set in form of branched or horsetail fracture pattern toward N-S direction (e.g., the Asmari anticline, Figure 9a). So, the main Miocene-Pliocene folding/thrusting event in the Zagros folded belt has been accommodated through both reactivation of previously formed vein sets and new fold-related fractures (Figure 14d). Other forms of fracture reactivations, including fracture intensifying and reorientation under locally perturbed stress field related to folding likely occurred in this phase. So, in the final fold geometry, and depending on the location of the fold in the studied area, different trends and types of microstructures are observed (Figure 14d).

6. Conclusion

[53] Our observations on fold geometries, deformation styles and vein populations in the Zagros indicate that most of the studied anticlines are not cylindrical and that conventional fold-related fracture models do not fully explain their fracturing style. An important finding of this study is that most extensional fractures observed in the field are mostly veins related to prefolding tectonics, and that they were later reactivated during folding. This study therefore supports the need of carefully considering prefolding joint/vein sets in realistic conceptual fold-fracture models as pointed out by *Bergbauer and Pollard* [2004] or *Bellahsen et al.* [2006].

[54] Another important point is that early basement block movements may have an impact on fracture development in the cover rocks. The vein sets striking N50°, N20° and N150° are widespread over the studied area: while the former presumably initiated during the earliest stage of the collisional stress build-up, the latter developed in the studied area in response to early flexure/forced-folding above NW-SE trending reactivated basement faults. The N-S and E-W vein systems also show a local concentration near the other major tectonic elements like N-S trending Izeh-Hendijan (IZHF) and Kharg-Mish (KMF) basement faults. Apparently, the occurrence of these vein sets was controlled either directly by underlying deep-seated basement faults and/or N-S trending preexisting folds in the Zagros region like the ones which exist beyond the Zagros deformation front. We conclude that the transmission of orogenic stress through the faulted crystalline basement of the Zagros was probably heterogeneous and complex in accordance with the overall transpressive setting of the studied area and the dispersion of vein set orientation described in this paper. For this reason, the deformation front probably propagated in an irregular fashion through the basement and the cover leading to a complex chronology of vein development in the cover. Such a complexity should be taken into account in further studies of folded and fractured reservoirs.

[55] On a regional point of view, the absolute dating of these early vein sets could be a key point toward a better definition of the timing of the onset of deformation in the Zagros; it would further allow discussion of the model of partitioning of the Arabia-Eurasia convergence in relation to the onset of motion of the MRF [*Talebian and Jackson*, 2004; *Agard et al.*, 2005] in the NW Zagros basin.

[56] Development of the low angle reverse faults and thrusts in the sedimentary cover is considered as the latest fracturing episode in the Central Zagros based on the conceptual model proposed in this paper. Shearing and reopening of pre-existing vein sets appears finally to be a very important mechanism to control the deformation within cover folds. It therefore comes that in the present-day folds of the Central Zagros, the different observed vein sets are the products of a long deformation history which started before the onset of the main stage of cover folding.

[57] **Acknowledgments.** The authors thank THE INTERNATIONAL IOR RESEARCH COOPERATION FOR IRANIAN FIELDS — A JOINT STUDY PROGRAM (IOR-JSP) for permission to publish this paper. This paper in part is based on two field surveys that were organized by the IOR-JSP project team for ''SEQUENCE STRATIGRAPHY AND STRUCTURAL GEOLOGY OF THE ASMARI FORMATIONS IN THE DEZFUL EMBAYMENT''. Fellow colleagues from various organizations of the National Iranian Oil Company (NIOC), Research Institute for Petroleum Industry (RIPI), IFP, CSIRO Petroleum, Petroware Pars (PWP), TOTAL, STATOIL, HYDRO, PETRONAS, and BP were actively involved in the said project. We also thank Nicolas Bellahsen for his advices and the two reviewers, D. Peacock and F. Storti, for their stimulating comments.

References

Abdollahie, F. I., A. Braathen, M. Mokhtari, and S. A. Alavi (2006), Interaction of the Zagros fold-thrust belt and the Arabian-type, deep-seated folds in the Abadan Plain and the Dezful Embayment, SW Iran, *Petrol. Geosci.*, *12*(4), 347–362.

Agard, P., J. Omrani, L. Jolivet, and F. Mouthereau (2005), Convergence history across Zagros, Iran; constraints from collisional and earlier deformation, *Geologische Rundschau = Int. J. Earth Sci. 1999. Print*, *94*(3), 401–419.

Ahmadhadi, F., O. Lacombe, and J. M. Daniel (2007), Early reactivation of basement faults in Central Zagros (SW Iran): evidence from pre-folding fracture populations in the Asmari Formation and Lower Tertiary paleogeography, in *Thrust Belts and Fore-*

land Basins; From Fold Kinematics to Hydrocarbon Systems, Frontiers in Earth Sciences, edited by O. Lacombe, J. Lavé, J. Vergès, and F. Roure, Springer Verlag, Chapter 11, 205–208.

Alavi, M. (1994), Tectonics of the Zagros orogenic belt of Iran: New data and interpretations, *Tectonophysics*, *229*(3–4), 211–238.

Allmendinger, R. W. (1982), Analysis of microstructures in the Meade Plate of the Idaho-Wyoming foreland thrust belt, U.S.A., *Tectonophysics*, *85*(3–4), 221–251.

Anastasio, D. J., D. M. Fisher, T. A. Messina, and J. E. Holl (1997), Kinematics of decollement folding in the Lost River Range, Idaho, *J. Struct. Geol.*, *19*(3–4), 355–368.

Bahroudi, A., H. A. Koyi, and C. J. Talbot (2003), Effect of ductile and frictional decollements on style of extension, *J. Struct. Geol.*, *25*(9), 1401–1423.

Bellahsen, N., P. Fiore, and D. D. Pollard (2006), The role of fractures in the structural interpretation of Sheep Mountain Anticline, Wyoming, *J. Struct. Geol.*, *28*(5), 850–867.

Berberian, M. (1983), The southern Caspian: A compressional depression floored by a trapped, modified oceanic crust, *Can. J. Earth. Sci.*, *20*(2), 163–183.

Berberian, M. (1995), Master 'blind' thrust faults hidden under the Zagros folds: Active basement tectonics and surface morphotectonics, *Tectonophysics*, *241*(3–4), 193–224.

Berberian, M., and G. C. P. King (1981), Towards a paleogeography and tectonic evolution of Iran, *Can. J. Earth. Sci.*, *18*(2), 210–265.

Bergbauer, S., and D. D. Pollard (2004), A new conceptual fold-fracture model including prefolding joints, based on the Emigrant Gap Anticline, Wyoming, *Geol. Soc. Am. Bull.*, *116*(3–4), 294–307.

Beydoun, Z. R. (1988), Petroleum habitat, northern Middle East: A review, *Bull. Houston Geol. Soc.*, *30*(7), 11.

Beydoun, Z. R. (1991), Arabian Plate hydrocarbon geology and potential: A plate tectonic approach, *AAPG Stud. Geol.*, *33*.

Blanc, E. J. P., M. B. Allen, S. Inger, and H. Hassani (2003), Structural styles in the Zagros simple folded zone, Iran, *J. Geol. Soc. London*, *160*(3), 401–412.

Colman-Sadd, S. P. (1978), Fold development in Zagros simply folded belt, Southwest Iran, *AAPG Bull.*, *62*(6), 984–1003.

Cooper, M. (1992), The analysis of fracture systems in surface thrust structures from the foothills of the Canadian Rockies, in *Thrust Tectonics*, edited by K. R. Mc Clay, 391–405, Chapman & Hall, London, United Kingdom.

Cooper, S. P., L. B. Goodwin, and J. C. Lorenz (2006), Fracture and fault patterns associated with basement-cored anticlines: The example of Teapot Dome, Wyoming, *AAPG Bull.*, *90*(12), 1903–1920.

Cosgrove, J. W., and M. S. Ameen (2000), A comparison of the geometry, spatial organization and fracture patterns associated with forced folds and buckle folds, *Geol. Soc. Spec. Pub.*, *169*, 7–21.

Couzens, B. A., and W. M. Dunne (1994), Displacement transfer at thrust terminations: The Saltville Thrust and Sinking Creek Anticline, Virginia, U.S.A., *J. Struct. Geol.*, *16*(6), 781–793.

Couzens-Schultz, B. A., B. C. Vendeville, and D. V. Wiltschko (2003), Duplex style and triangle zone formation: Insights from physical modeling, *J. Struct. Geol.*, *25*(10), 1623–1644.

Dahlstrom, C. D. A. (1990), Geometric constraints derived from the law of conservation of volume and applied to evolutionary models for detachment folding, *AAPG Bull.*, *74*(3), 336–344.

DeMets, C., R. G. Gordon, D. F. Argus, and S. Stein (1990), Current plate motions, *Geophys. J. Int.*, *101*(2), 425–478.

Engelder, T. (1987), Joints and shear fractures in rock, in *Fracture Mechanics of Rocks*, Geology Series, edited by B. K. Atkinson, 27–69, Academic Press.

Erslev, E. A., and K. R. Mayborn (1997), Multiple geometries and modes of fault-propagation folding in the Canadian thrust belt, *J. Struct. Geol.*, *19*(3–4), 321–335.

Falcon, N. L. (1961), Major earth-flexuring in the Zagros mountains of south-west Iran, *Q. J. Geol. Soc. London*, *117*(468), 367–376.

Falcon, N. L. (1974), Southern Iran: Zagros Mountains, *Geol. Soc. Spec. Pub.*, *4*, 199–211.

Favre, N. L. (1975), Structures in the Zagros orogenic belt, OSCO.

Fisher, D. M., and D. J. Anastasio (1994), Kinematic analysis of a large-scale leading edge fold, Lost River Range, Idaho, *J. Struct. Geol.*, *16*(3), 337–354.

Fischer, M. P., N. B. Woodward, and M. M. Mitchell (1992), The kinematics of break-thrust folds, *J. Struct. Geol.*, *14*(4), 451–460.

Gholipour, A. M. (1998), Patterns and structural positions of productive fractures in the Asmari reservoirs, Southwest Iran, *J. Can. Petr. Tech.*, *37*(1), 44–50.

Graham Wall, B. R., R. Girbacea, A. Mesonjesi, and A. Aydin (2006), Evolution of fracture and fault-controlled fluid flow pathways in carbonates of the Albanides fold-thrust belt, *AAPG Bull.*, *8*, 1227–1249.

Haynes, S. J., and H. McQuillan (1974), Evolution of the Zagros Suture Zone, Southern Iran, *Geol. Soc. Am. Bull.*, *85*(5), 739–744.

Hennings, P. H. (2000), Combining outcrop data and three-dimensional structural models to characterize fractured reservoirs: An example from Wyoming, *AAPG Bull.*, *84*(6), 830.

Hessami, K., H. A. Koyi, and C. J. Talbot (2001), The significance of strike-slip faulting in the basement of the Zagros fold and thrust belt, *J. Petrol. Geol.*, *24*(1), 5–28.

Hull, C. E., and H. R. Warman (1970), Asmari oil fields of Iran, *AAPG Mem.*, *14*, 428–437.

Jackson, J. (1980), Errors in focal depth determination and the depth of seismicity in Iran and Turkey, *Geophys. J. R. Astron. Soc.*, *61*(2), 285–301.

Jackson, J. (1987), Active normal faulting and crustal extension, in *Continental Extension*, vol. 28, edited by M. P. Coward, J. F. Dewey, and P. L. Hancock, 3–19, Geol. Soc. London.

Jackson, J., and D. McKenzie (1984), Rotational mechanisms of active deformation in Greece and Iran, *Geol. Soc. Spec. Pub.*, *17*, 743–754.

James, G. A., and J. G. Wynd (1965), Stratigraphic nomenclature of Iranian Oil Consortium Agreement Area, *AAPG Bull.*, *49*(12), 2182–2245.

Jamison, W. R. (1997), Quantitative evaluation of fractures on Monkshood Anticline, a detachment fold in the foothills of Western Canada, *AAPG Bull.*, *81*(7), 1110–1132.

Kittler, J. (1976), A locally sensitive method for cluster analysis, *Pattern Recognition*, *8*, 23–33.

Koyi, H. A., and B. C. Vendeville (2003), The effect of decollement dip on geometry and kinematics of model accretionary wedges, *J. Struct. Geol.*, *25*(9), 1445–1450.

Lacombe, O., and F. Mouthereau (2002), Basement-involved shortening and deep detachment tectonics in forelands of orogens: insights from recent collision belts (Taiwan, western Alps, Pyrenees), *Tectonics*, *21*(4), 1030, doi:10.1029/2001TC901018.

Lees, G. M. (1952), Foreland folding, *Q. J. Geol. Soc. London*, *108*(429), 1–34.

Letouzey, J., S. Sherkati, J. M. Mengus, H. Motiei, M. Ehsani, A. Ahmadnia, and J. L. Rudkiewicz (2002), A regional structural interpretation of the Zagros mountain belt in northern Fars and high Zagros (SW Iran), *Annual Meeting Expanded Abstracts - American Association of Petroleum Geologists*, *2002*, 102.

Lisle, R. J. (2000), Predicting patterns of strain from three-dimensional fold geometries: Neutral surface folds and forced folds, *Geol. Soc. Spec. Pub.*, *169*, 213–221.

Marcotte, D., and E. Henry (2002), Automatic joint set clustering using a mixture of bivariate normal distributions, *Int. J. Rock. Mech. Min. Sci.*, *39*, 323–334.

McClusky, S., R. Reilinger, S. Mahmoud, D. Ben Sari, and A. Tealeb (2003), GPS constraints on Africa (Nubia) and Arabia plate motions, *Geophys. J. Int.*, *155*(1), 126–138.

McQuillan, H. (1973), Small-scale fracture density in Asmari Formation of Southwest Iran and its relation to bed thickness and structural setting, *AAPG Bull.*, *57*(12), 2367–2385.

McQuillan, H. (1974), Fracture patterns on Kuh-e Asmari anticline, Southwest Iran, *AAPG Bull.*, *58*(2), 236–246.

Motiei, H. (1993), Geology of Iran, Zagros Stratigraphy, *Geological Society of Iran Publications*.

Motiei, H. (1995), Petroleum Geology of Zagros, 1 & 2, *Geological Society of Iran Publications*, 1009 p.

Mouthereau, F., O. Lacombe, and B. Meyer (2006), The Zagros folded belt (Fars, Iran): Constraints from topography and critical wedge modelling, *Geophys. J. Int.*, *165*(1), 336–356.

Mouthereau, F., J. Tensi, N. Bellahsen, O. Lacombe, T. Deboisgrollier, and S. Kargar (2007), Tertiary sequence of deformation in a thin-skinned/thick-skinned collision belt: The Zagros Folded Belt (Fars, Iran), *Tectonics*, *26*, TC5006, doi:10.1029/2007TC002098.

Ni, J., and M. Barazangi (1986), Seismotectonics of the Zagros continental collision zone and a comparison with the Himalayas, *J. Geophys. Res*, *91*(B8), 8205–8218.

Peacock, D. C. P., and D. J. Sanderson (1995), Pull-aparts, shear fractures and pressure solution, *Tectonophysics*, *241*, 1–13.

Pollard, D., and A. Aydin (1988), Progress in understanding jointing over the past century, *Geol. Soc. Am. Bull.*, *100*, 1181–1204.

Price, N. J., and J. W. Cosgrove (1990), Analysis of geological structures, *Cambridge Univ. Press*.

Sattarzadeh, Y., J. W. Cosgrove, and C. Vita-Finzi (2000), The interplay of faulting and folding during the evolution of the Zagros deformation belt, *Geol. Soc. Spec. Pub.*, *169*, 187–196.

Sepehr, M., and J. W. Cosgrove (2004), Structural framework of the Zagros Fold-Thrust Belt, Iran, *Mar. Pet. Geol.*, *21*(7), 829–843.

Sepehr, M., J. W. Cosgrove, and M. P. Coward (2002), The major fault zones controlling the sedimentation, deformation and entrapment of hydrocarbon in the Zagros fold-thrust belt, Iran, *Annual Meeting Expanded Abstracts - American Association of Petroleum Geologists*, *2002*, 160–161.

Sherkati, S., and J. Letouzey (2004), Variation of structural style and basin evolution in the central Zagros (Izeh Zone and Dezful Embayment), Iran, *Mar. Pet. Geol.*, *21*(5), 535–554.

Sherkati, S., J. Letouzey, and D. Frizon de Lamotte (2006), Central Zagros fold-thrust belt (Iran): New insights from seismic data, field observation and sandbox modeling, *Tectonics*, *25*, TC4007, doi:10.1029/2004TC001766.

Silliphant, L. J., T. Engelder, and M. R. Gross (2002), The state of stress in the limb of the Split Mountain anticline, Utah: Constraints placed by transected joints, *J. Struct. Geol.*, *24*, 155–172.

Srivastava, D. C., and T. Engelder (1990), Crack-propagation sequence and pore-fluid conditions during fault-bend folding in the Appalachian Valley and Ridge, central Pennsylvania, *Geol. Soc. Am. Bull.*, *102*(1), 116–128.

Stearns, D., and M. Friedman (1972), Reservoirs in fractured rocks, in *Stratigraphic Oil and Gas Fields*, AAPG Memoir, vol. 16, 82–106.

Stoecklin, J. (1968), Structural history and tectonics of Iran: A review, *Am. Assoc. Petrol. Geologists Bull.*, *52*(7), 1229–1258.

Storti, F., and F. Salvini (2001), The evolution of a model trap in the Central Apennines, Italy: Fracture patterns, fault reactivation and development of cat-

aclastic rocks in carbonates at the Narni Anticline, *J. Pet. Geol.*, *24*(2), 171–190.

Talbot, C. J., and M. Alavi (1996), The past of a future syntaxes across the Zagros, *Geol. Soc. Spec. Pub.*, *100*, 89–109.

Talebian, M., and J. Jackson (2002), Offset on the main recent fault of NW Iran and implications for the late Cenozoic tectonics of the Arabia-Eurasia collision zone, *Geophys. J. Int.*, *150*(2), 422–439.

Talebian, M., and J. Jackson (2004), A reappraisal of earthquake focal mechanisms and active shortening in the Zagros Mountains of Iran, *Geophys. J. Int.*, *156*(3), 506–526.

Tavani, S., F. Storti, O. Fernandez, J. A. Munoz, and F. Salvini (2006), 3-D deformation pattern analysis and evolution of the Anisclo anticline, southern Pyrenees, *J. Struct. Geol.*, *28*, 695–712.

Thorbjornsen, K. L., and W. M. Dunne (1997), Origin of a thrust-related fold; geometric vs kinematic tests, *J. Struct. Geol.*, *19*(3–4), 303–319.

Vernant, P., and J. Chery (2006), Mechanical modelling of oblique convergence in the Zagros, Iran, *Geophys. J. Int.*, *165*(3), 991–1002.

Vernant, P., F. Nilforoushan, D. Hatzfeld, M. R. Abbassi, C. Vigny, F. Masson, H. Nankali, J. Martinod, A. Ashtiani, R. Bayer, F. Tavakoli, and J. Chery (2004), Present-day crustal deformation and plate kinematics in the Middle East constrained by GPS measurements in Iran and northern Oman, *Geophys. J. Int.*, *157*(1), 381–398.

Wennberg, O. P., T. Svånå, M. Azizzadeh, A. M. M. Aqrawi, P. Brockbank, K. B. Lyslo, and S. Ogilvie (2007), Fracture intensity vs. mechanical stratigraphy in platform topcarbonates: The Aquitanian of the Asmari Formation, Khaviz Anticline, Zagros, SW Iran, *Pet. Geosci.*, *12*, 235–245.

Whitaker, A. E., and T. Engelder (2005), Characterizing stress fields in the upper crust using joint orientation distributions, *J. Struct. Geol.*, *27*(10), 1778.

Wollmer, F. W. (1995), C Program for automatic contouring of spherical orientation data using a modified Kamb method, *Comput. Geosci.*, *21*, 21–49.

Woodcock, N. H. (1977), Specification of fabric shapes using an eigenvalue method, *Geol. Soc. Am. Bull.*, *88*(9), 1231.

F. Ahmadhadi, Iranian Offshore Oil Company (IOOC), IOOC Tower - 12th Floor, Geology & Petrophysics Department, #38, Tooraj St., Vali-e-asr Ave., Chamran Crossing (Park-vey), Tehran 19395, Iran.

M. Azzizadeh, RIPI, West Blvd., Azadi Sport Complex, P.O. Box 14665-1998, Tehran, Iran.

J.-M. Daniel, Institut Français de Pétrole (IFP), 1 et 4, Rue de Bois-Préau, 92506 Rueil-Malmaison Cedex, France. (j-marc.daniel@ifp.fr)

O. Lacombe, Université P. & M. Curie - Paris 6, Laboratoire de Tectonique, UMR 7072 CNRS, T46-45, E2, Case 129, 4 place Jussieu, F-75252 Paris Cedex 05, France.